HHS Public Access

Author manuscript

Matter. Author manuscript; available in PMC 2021 October 07.

Published in final edited form as:

Matter. 2020 October 7; 3(4): 1087–1113. doi:10.1016/j.matt.2020.08.002.

Bioinspired Materials for *In Vivo* Bioelectronic Neural Interfaces

Grace A. Woods[1,3], **Nicholas J. Rommelfanger**[1,3], **Guosong Hong**[2,3,*]

[1]Department of Applied Physics, Stanford University, Stanford, California, 94305, USA

[2]Department of Materials Science and Engineering, Stanford University, Stanford, California, 94305, USA

[3]Wu Tsai Neurosciences Institute, Stanford University, Stanford, California, 94305, USA

Abstract

The success of *in vivo* neural interfaces relies on their long-term stability and large scale in interrogating and manipulating neural activity after implantation. Conventional neural probes, owing to their limited spatiotemporal resolution and scale, face challenges for studying the massive, interconnected neural network in its native state. In this review, we argue that taking inspiration from biology will unlock the next generation of *in vivo* bioelectronic neural interfaces. Reducing the feature sizes of bioelectronic neural interfaces to mimic those of neurons enables high spatial resolution and multiplexity. Additionally, chronic stability at the device-tissue interface is realized by matching the mechanical properties of bioelectronic neural interfaces to those of the endogenous tissue. Further, modeling the design of neural interfaces after the endogenous topology of the neural circuitry enables new insights into the connectivity and dynamics of the brain. Lastly, functionalization of neural probe surfaces with coatings inspired by biology leads to enhanced tissue acceptance over extended timescales. Bioinspired neural interfaces will facilitate future developments in neuroscience studies and neurological treatments by leveraging bidirectional information transfer and integrating neuromorphic computing elements.

eTOC blurb:

Bioelectronic neural interfaces have afforded unprecedented opportunities to understand information processing in the brain and treat neurological disorders. Despite decades of effort, the design of conventional neural interfaces generally bears little resemblance to the properties of the neural tissue they are designed to interface. In this review, we emphasize the importance of leveraging bioinspired properties at the brain-device interface. Specifically, we classify four

*Correspondence should be addressed to guosongh@stanford.edu.

Author contributions

Writing – Original Draft, G.A.W.; Writing – Review & Editing, G.A.W., N.J.R. and G.H

Declaration of interests

The authors declare no competing interests.

properties for next-generation bioelectronic neural interfaces to emulate: size and morphology, mechanics, topology, and biochemical functionalization.

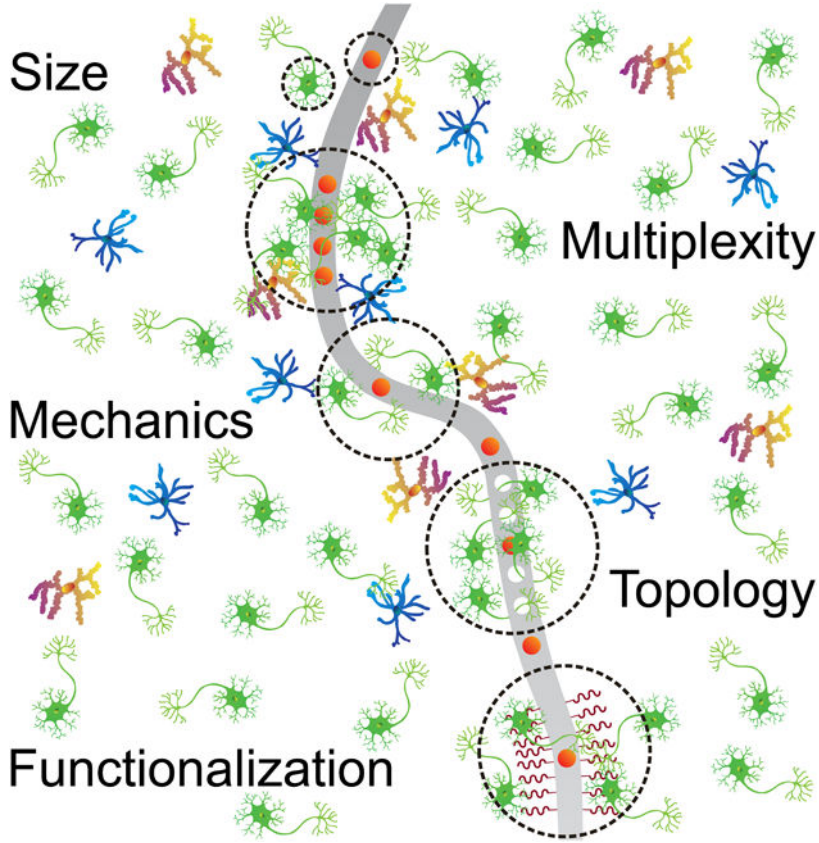

Keywords

Biomimetics; brain-machine interfaces; nanoelectronics; tissue-like electronics; neural recording; neural stimulation; neural probes; brain implants; chronic stability; spatiotemporal resolution

Materials innovations have constantly driven the development of neural interfaces that allow neuroscientists to advance our understanding of the brain and enable neurologists to treat a variety of brain disorders.[1–4] Scientific inquiry on the relationship between behaviors and their underlying neural circuits arguably began in the late 18th century, when Galvani demonstrated the ability of electrical stimuli to evoke motor output.[5] His experiment, which laid the foundation for electrophysiology, routed a frog's spinal cord to its thigh with an iron and bronze arch, producing the first electrical interface to stimulate the nerve. In the 19th century, scientists established direct connection between the brain and motor output by stimulating a dog's cerebrum with a platinum wire and observing the corresponding limb movement.[6] The field initiated by these early experiments has since produced electrical therapies such as deep-brain stimulation (DBS), arguably one of the most successful neurotechnologies for translational medicine, offering relief for debilitating neurological conditions such as Parkinson's disease, epilepsy, and dystonia.[7, 8] Despite its profound clinical impact, modern DBS electrodes are relatively large and rigid rods comprising

platinum-iridium (PtIr) or stainless steel electrodes.[9] Therefore, conventional neuromodulation electrodes are similar in material design and properties to the metallic arch used in Galvani's experiment more than two centuries ago,[10] while bearing little resemblance to the structure and properties of the neural tissue they are designed to interface.

Besides the neural interfaces that stimulate activity in neural tissue, neural recording interfaces, which afford information flow in the opposite direction, have traditionally been constructed with similar materials. In 1957, Hubel developed an electrolytically sharpened tungsten wire for direct recording of extracellular action potentials at the single neuron level, demonstrating reliable recording in a feline brain for up to 1 hour.[11] These tungsten electrodes have since received widespread use in both neuroscience and neurology studies.[12] Shortly thereafter, the patch clamp technique was developed to resolve neuronal behavior at the level of individual ion channels.[13] By taking advantage of glass thermal drawing methods, the patch clamp technique involves elongating glass into a tapered micropipette, with a tip fine enough to perturb a small number of ion channels without affecting the entire cell.[14] However, the patch clamp technique requires substantial insulation from vibration and reduction in shunt conductance to resolve neural signals.[15] It is noteworthy that intracellular recordings by patch clamp are usually obtained from one cell at a time under non-physiological conditions, such as cultured neurons, tissue slices, and anesthetized brains.[16] *In vivo* extracellular recording electrodes, such as the tungsten wire electrodes pioneered by Hubel, provide a proxy of the intracellular membrane potential waveform, which has been confirmed by simultaneous recordings of both intracellular and extracellular signals using separate electrodes[16] or the same neural probe.[17] In the 1970's and 1980's, advancements in semiconductor fabrication provided the foundation for silicon-based microelectrode arrays (MEAs).[18] The Michigan array, with multiple recording electrodes per silicon shank, and the Utah array, featuring a two-dimensional (2D) array with micron-sized metal-plated silicon tips as recording sites, enabled scientists to probe neural circuitry with multi-site throughput and single-unit resolution, significantly improving neurotechnology standards.[19–22] Similar to DBS electrodes, these recording devices are designed and fabricated with large and rigid non-biological features that prevent intimate interfacing over extended time periods with the endogenous neural tissue.

These foundational neural interfaces, both for stimulation and recording of neural activity, laid the framework for emergent bioelectronic neural probes with more desirable, bioinspired design features.[18, 23, 24] The efficacy of neural probes is contingent on how well the device conforms to and interfaces with the local brain environment – both with its feature sizes and with its mechanical, topological, and biochemical properties.[25, 26] Mismatch in these properties, where poor device design and material choices aggravate the inherent device-brain interaction, results in failure modes such as irreversible device degradation, inflammation-induced gliosis, neuron death and the subsequent loss of recorded neural signals and stimulation capability over a chronic timescale.[27, 28] For example, DBS electrodes suffer from significant glial scarring at the device-tissue interface as a result of implant size and mechanical mismatch.[29] Conventional neural recording interfaces, such as the Michigan and Utah arrays, also suffer from chronic recording instability as a result of glial scarring and mechanical mismatch with the neural tissue.[27, 28]

We argue that the challenges faced by existing bidirectional neural interfaces are a direct consequence of designs that have been historically developed without an *a priori* understanding of the nervous system.[30] It has been demonstrated that neurotechnology design principles should match the brain's known properties to optimize recording stability, resolution, and signal-to-noise ratio (SNR).[2, 31] By taking inspiration from the brain and biology, there exists a rich opportunity to develop bidirectional neural interfaces which seamlessly integrate with the brain environment. In particular, the focus of this review is to define and demonstrate several principal properties of modern neurotechnology to optimize bidirectional transfer of neural information, based on fundamentally new structural, mechanical, topological, and biochemical design principles inspired by biology. Specially, we highlight the following key features of the nervous system (Fig. 1A) that have constantly inspired the evolution of emerging neural interfacing technologies (Table 1 & Fig. 2):

1. Size and morphology (Fig. 1B&C)
2. Mechanical properties (Fig. 1D)
3. Topology (Fig. 1E)
4. Biochemical functionalization (Fig. 1F)

Bioinspired Size and Morphology

In the late 19th century, Ramón y Cajal utilized the Golgi staining method to illuminate the underlying complexity of the composition and connections within the brain.[74] The stunningly exquisite drawings of Ramón y Cajal revealed the largely heterogenous structure of neurons (unlike many other somatic cells), comprising feature sizes that span many orders of magnitude and structures vastly different in their shapes and aspect ratios. For example, neuron somata range from 1 to 20 μm in size,[32] axonal diameters range from 0.16 to 9 μm (with a high aspect ratio),[33] and synaptic cleft distances range from 20 to 40 nm.[75] Early-stage bioelectronic neural interfaces were limited by their large feature sizes, which showed great disparity from the characteristic sizes of neurons and sub-neuronal structures. Consequently, in vertebrate nervous systems, these devices were exclusively capable of measuring collective neuronal behavior, such as LFPs common in synchronous brain function.[76] Single-neuron activity was measured only in invertebrate nervous systems with these devices, such as squid giant axons with millimeter diameters.[77] Since the 1950's, neural probes have established a paradigm for minimizing size (Fig. 1B) and increasing packing density of electrodes (Fig. 1C) through advancements in device fabrication strategies, such as photolithography, electron-beam lithography (EBL), and micromachining. For example, deep ultraviolet (DUV) photolithography is able to produce feature sizes down to 50 nm,[78] EBL has been reported to achieve feature sizes down to 2 nm,[79] and micromachining can achieve high precision typically better than 1 μm.[80] This strategy has enabled the measurement of extracellular single-unit neuron activity from the mammalian brain by making the recording electrodes similar in size and density to the neurons they are designed to measure. Our ability to understand the connection between brain activity and behavior ultimately relies on improving the resolution and fidelity of next-generation bioelectronic neural probes inspired by the size and morphology of individual neurons.

Reducing the feature sizes of bioelectronic neural interfacing devices improves the resolution of measured neuronal behavior by decreasing the likelihood of signal attenuation though spatial averaging.[81] For example, a simulated signal measured 1 μm away by a 1×1 μm^2 electrode was reduced by 95% in signal amplitude when measured by a 100×100 μm^2 electrode at the same distance.[81] However, reduction of feature sizes is simultaneously demanding of applicable materials and fabrication methods. This challenge directly results from the fundamental difference in the bottom-up and top-down approaches that nature and engineers use to create functional devices, respectively.[82] Traditionally, top-down fabrication technologies are used in engineering of neural interfaces, such as the electropolishing method used for Hubel's tungsten microwire electrodes,[11] and micromachining and photolithography for making silicon-based Michigan/Utah arrays.[19, 20] The same top-down approaches have been used for fabricating the state-of-the-art high-density Michigan array, Neuropixels.[57] In contrast, although widely found in biology, bottom-up approaches were employed to a lesser degree in engineering until recent years. For example, bioelectronic neural interfaces have been demonstrated with synthesized kinked silicon nanowires for extracellular and intracellular *in vitro* recordings of electrogenic cells.[83, 84] In addition, free standing kinked nanowires and U-shaped nanowires, which integrate both bottom-up (nanowire synthesis) and top-down (lithographic patterning and assembly) approaches, have been demonstrated for enhanced cell targeting and multiplexing for *in vitro* intracellular recording of cardiomyocytes and neurons.[68, 85, 86] Despite these examples demonstrating the feasibility of bottom-up bioelectronic neural devices, bottom-up processing generally limits the complexity, reproducibility, and scalability of devices with small feature sizes.[87] Therefore, it is essential to judiciously design bioelectronic neural probes with reduced feature sizes and improved spatial resolution.

The maturation of fabrication technologies and materials discovery significantly refined the resolution of modern neural interface design to approach the feature sizes of individual neurons and their subcellular components (Fig. 3A). Modern neural interfaces now use a range of manufacturing techniques, from EBL to polymer-based thermal drawing processes used to create multifunctional probes.[50, 88, 89] EBL offers a higher patterning resolution than photolithography, as the feature resolution of photolithography is limited by UV diffraction (approximately the wavelength of light used, ranging from 50 nm to ~1 μm),[78] while the resolution of electron-beam lithography is often limited by the secondary electrons generated by the interaction between photoresist and the electron beam (typically ~tens of nm).[90] In comparison, thermal drawing processing allows for high-throughput manufacturing of bioelectronic devices with up to a 200× reduction in cross-sectional area, producing electrode cross-sectional areas down to 5 μm via manufacturing of materials with similar glass and melting temperatures (Fig. 2A & Fig. 3B, **i**).[50] Below, we highlight two bioinspired approaches to address such challenges: bioelectronic neural interfaces with feature sizes approaching individual neurons and with morphology mimicking neurites.

Feature sizes approaching individual neurons

By constructing electronic devices with densely packed electrodes of similar size to that of a neuron soma, ranging from 1 – 20 μm, an intimate neural tissue-probe interface can be realized at the single-neuron level with a significantly increase in electrode density and

multiplexity.[57, 73] This strategy has been demonstrated in a range of modern neural probes recently, including the multifunctional fibers (Fig. 2A, Fig. 3B, **i**),[50] NeuroGrid (Fig. 2B),[52] ultraflexible nanoelectronic probe (Fig. 2F, Fig. 3B, **ii**),[56] Neuropixels (Fig. 2E, Fig. 3B, **iii**),[57] NeuroRoots (Fig. 2G, Fig. 3B, **iv**),[61] and neuron-like electronics (NeuE, Fig. 2H, Fig. 3B, **v**).[63] For example, NeuroGrid offers an approach to record both collective and single-unit neural signals from the brain's cortical surface in an electrocorticography (ECoG) setting (Fig. 2B).[52] Inspired by the size and spacing of neurons in the cortex, NeuroGrid is designed with 10×10 μm^2 electrodes and 30 μm interspacing, resolving both LFPs and action potentials from single neurons without brain penetration. In a further development, the enhancement-mode ion-gated transistor (e-IGT) with a channel length of 5 μm provides high speed and high gain for electrophysiological recordings performed with low power consumption owing to the default OFF state at zero gate potential. The combination of the enhancement mode and the conventional depletion mode achieves internal filtering in a wide voltage range to suit electromyography, electrocardiography, intracranial encephalography, and action potential measurements.[71] In a recent example of a flexible, multiplexed electrode array called "Neural Matrix", ECoG signals were recorded from 1,008 channels over a year in duration and a centimeter-scale brain region in space.[70]

The strategy of reducing electrode size to approach individual neurons and thus affording a high channel count of single-unit recording has also been adapted in the implantable neural probes. For example, the Neuropixels array (Fig. 2E, Fig. 3B, **iii**) represents a significant upgrade in channel count to similar silicon-based intracranial neural interfaces, such as the Michigan array. The Neuropixels array utilizes 130 nm CMOS technology[91] and is now a consumer standard for high electrode density and small feature size neural interfaces with its 960 12×12 μm^2 electrodes placed on a 70×20 μm^2 shank.[57] Meanwhile, the Argo system, a highly multiplexed Utah-like array, provides the highest channel count *in vivo* neural recording system to date, affording simultaneous recording from its 65,536 channels.[73]

Finally, building devices with inspiration from synapses and single ion channels wields the power to elucidate the behavior of subthreshold neural activity, such as transmembrane dynamics of individual ion channels. Ultrashort-channel nanowire field-effect transistors (FETs) with a 50 nm channel length and sub-10 nm branched intracellular nanotube field-effect transistors (BIT-FETs), mimicking the size of single ion channels, offer an alternative to patch clamp for recording from individual ion channels with subcellular resolution (Fig. 3C, **vi** & **vii**).[49, 68, 86, 92] The impedance of ultrashort FETs and BIT-FETs with sizes down to <10 nm is significantly lower than would be anticipated with decreasing micropipette size in the patch clamp technique. This is enabled by the devices' independence from interfacial impedances, allowing higher signal-to-noise recording of transmembrane potential with the capability to increase the multiplexity (i.e., channel count) of subcellular recording.[93] Progress has also been made to the conventional patch clamp techniques. In a recent example, flexible quartz nanopipettes offer an alternative approach to conventional glass microelectrodes by featuring a reduced tip diameter of ~ 10 – 20 nm, which affords improved resolution and SNR for intracellular recordings (Fig. 3C, **viii**).[67]

Mimicking morphology of neurites

With a different perspective, neural probes inspired by the morphology of neurites and non-neuronal cells have also shown improved acceptance into the brain. This strategy has been demonstrated earlier in non-electronic neural tissue scaffolds, recognizing the importance of myelination of displaced axonal fibers in improving the longevity of neural probes in the brain.[94, 95] For example, inspired by the elongated morphology of axons, Lee et al. optimized a neural scaffold containing axon-like polystyrene nanofibers to optimize oligodendrocyte myelination.[96] The study uncovered the impact of polystyrene nanofiber diameters ranging from 0.2 – 4.0 μm on myelination efficiency, and unearthed the optimal range of diameters of polystyrene nanofiber for promoting myelination (greater than or equal to 0.5 μm). Typical axonal diameters fall within the range discovered in their results, suggesting that mirroring the morphology of neurites improves both the restoration of the endogenous neural tissue environment and the device-tissue acceptance. In addition, imitating the structural features of neurites has been demonstrated to improve the interface of neural tissue with electrophysiological neural probes in chronic studies. For example, NeuroRoots, a thread-like bioelectronic neural interface with small feature sizes, was designed with inspiration from the size and distribution of axonal bundles within the brain (Fig. 2G, Fig. 3B, **iv**).[61] With 10 μm diameter circular electrode pads and 7×1.5 μm^2 leads, NeuroRoots affords chronic recording stability up to 7 weeks and represents a promising technology to interrogate and modulate the firing of specific subpopulations of neurons in behaving animals. Similarly, Neurotassels offers a scalable, high electrode-density, and small-footprint approach to high-resolution and chronic recording stability devices, with sizes approaching those of neurites.[64] With a bioresorbable polymer coating comprising polyethylene glycol (PEG), Neurotassels self-assembles prior to insertion through elastocapillary interactions with a molten, tissue-dissolvable polymer. Another demonstration of a bioelectronic neural interface which is indistinguishable from the endogenous neural tissue is the bioinspired NeuE. By mirroring both the morphology and size of neuron somata and neurites, NeuE affords exceptional chronical stability for long-term brain interfacing (Fig. 2H, Fig. 3B, **v**). With recording electrodes mimicking the soma of typical pyramidal neurons (8 – 20 μm) and interconnect lines along with insulating ribbons mimicking axons and dendrites (width = 1 – 4 μm), NeuE allows high-resolution recording and encourages neural progenitor cell (NPC) migration.[63] The rostral migratory stream (RMS) is an endogenous structure in the rodent brain comprised of highly aligned vascular and glial cells which is dedicated to encouraging NPC migration.[97] As its role and structure become increasingly understood, there is a significant opportunity for next-generation bioelectronic devices to explicitly mimic the role of the RMS, as has been demonstrated in the NeuE probe, to further persuade brain-device compliance. Therefore, mimicking the cellular and subcellular anatomy of neurons and other cells has demonstrated increased bioelectronic neural interface acclimation and improved recording stability and resolution.

To conclude this section, we posit that feature size reduction and size- and morphology-mimicking of neurons and neurites imparts the following advantages on neural interface functionality:

1. High resolution of interfacing: Neural interfaces are capable of measuring single-unit activity in addition to LFPs, as electrodes approach the size of neural somata (Fig. 1B).
2. High density multiplexing: Due to modern manufacturing techniques and as a direct consequence of smaller electrodes, neural interfaces are constructed with orders of magnitude more electrodes while occupying the same, or even smaller, volume (Fig. 1C).
3. Improved axon myelination and progenitor cell migration: By reducing interconnect widths and mimicking the morphology of neurites and glial cells, neural interfaces encourage acceptance into the brain by promoting their interactions with neurons and non-neuronal cells.

Bioinspired Mechanical Properties

Failure modes of electrical neural probes generally arise from design flaws such as material-degradation or shorting,[98] and/or from device-brain interactions.[99] While design limitations of bioelectronic neural interfaces are largely addressed by modern fabrication and materials technologies, deleterious device-brain interactions remain a significant challenge to chronic interfacing with neural tissue. Effects of device-brain interactions may emerge as early as insertion (e.g., puncturing blood vessels and displacing neural tissue), or later during chronic interfacing due to an inherent mechanical property mismatch (e.g., neuronal death during relative motion and micromotion, or device insulation due to glial sheath).[100] We argue that the failure modes of implantable bioelectronic neural devices fundamentally arise from the mechanical property mismatch between neural interfaces and surrounding neural tissue.

Neural tissue is extremely soft, with its Young's modulus ranging from 100 Pa to 10 kPa.[101] This is a direct result of the composition of the neural tissue and the functions the tissue must fulfill: in order to transmit neural signals (in the form of membrane potentials) between different brain regions, the cable theory of neurites prescribes that the interior of the neurites must be conductive, while the exterior must be insulating.[102] Ionic solution is an ideal conductive material a neurite can use for its interior, while myelinating glial cells with rich membrane lipid content are a readily available insulating material for its exterior.[34] Both water and lipids are very fluidic, thus leading to the exceptional softness of the neural tissue.

Neural devices, however, are usually fabricated with much stiffer materials than the neural tissue, leading to mechanical mismatch which becomes the main contributor to the limited longevity and stability of a neural interface.[101] Two physical properties evaluate the mechanical compliance of a neural probe: the Young's modulus of the materials, and the bending stiffness of the structure. On one hand, Young's modulus is an intrinsic material property that measures the ability of a material to resist a change in length under tensile or compressive forces.[103] Typical materials used in neural interfaces are rigid, with Young's moduli 8 – 9 orders of magnitude larger than that of the brain.[1, 18] On the other hand, the bending stiffness measures the ability of a structure to resist bending deformation to applied force. Although the Young's modulus defines a material's intrinsic mechanical properties, the bending stiffness highlights the mechanical interaction between devices with certain

structures and the surrounding neural tissue (Fig. 1D), which affects the magnitude of neural tissue damage and the evoked chronic immune responses.[1, 18]

When the bending stiffness of bioelectronic neural implants exceeds that of neural tissue, a cascade of coupled chronic immune responses occur, ranging from the development of a local insulating glial sheath that renders electronic devices inoperable, to complete neuronal death.[27] Determining the origin of chronic immune responses is a complex problem, but it is known that a major source derives from the inertial difference between neural implants and surrounding tissue during micromotion (e.g., due to local blood flow and global motion).[2] Studies have demonstrated that softer and smaller devices have the potential to minimize chronic immune responses;[104] therefore, next-generation bioelectronic neural interfaces must be judiciously designed with materials and features with reduced mechanical mismatch to optimize chronic interfacing.

To improve mechanical compliance via a reduction of bending stiffness, which is proportional to the dominant material's Young modulus and feature sizes (Eqn. 1), next-generation bioelectronic device design must incorporate small size with softer materials. This design principle is governed by the dependence of effective bending stiffness (K; normalized against the width of the neural probe) on the Young's modulus and thickness of the neural probe:

$$K \alpha Ed^3 \quad \#(1)$$

where E and d are the Young's modulus and dimension in the direction of bending, respectively. Neural implants with significantly reduced bending stiffness can thus be achieved by reducing Young's modulus and/or reducing feature sizes (e.g., thickness). However, challenges remain in the design and fabrication of bioelectronic neural interfaces with similar mechanics to those of the neural tissue, since conventional technologies for making high-performance electronic systems usually use materials that are not mechanically compliant with the nervous tissue. Therefore, advances are needed in the constituent materials, architectural dimensions, and integration methods to impart bioinspired mechanical properties in next-generation neural interfaces.[4]

Softer materials reduce bending stiffness

Compared to hard materials such as silicon, polymers are ideal materials for neural probes owing to their low Young's modulus and thus high flexibility (Fig. 4A). For example, polyimide provides a flexible material for the insulating layer of neural probes and can be patterned via standard photolithography methods[105] and a novel laser-engraving method.[106] By encapsulating gold electrodes and interconnects in a polyimide substrate, Rousche et al. introduced a new direction for neural interfaces by combining flexibility, biocompatibility, and chronic recording stability. The first generation of polyimide probes demonstrated chronic recording stability of multiunit neural activity, with a SNR of ~5.[42] A multitude of neural interfaces with various polymer-based materials, shapes, and topologies have since been developed and demonstrated evidence for improved chronic compliance. NeuroGrid combines ultrathin and highly conformable materials (4 μm, parylene C) with its bioinspired architecture, described in the previous section, and demonstrates stable recordings for up to

10 days.[52] Similarly, a device designed to mimic the properties of the dura mater, called the e-dura, combines silicone, gold interconnects, and soft Pt-silicone composite electrodes into a flexible package (Fig. 2C).[51] By comparing the e-dura with a rigid device, the authors noted significant improvements in motor performance, decreased spinal cord damage, and lessened microglial and astrocytic accumulation after 6 weeks. In addition, multifunctional fibers, which leverage polymers alone to form optical waveguides, conductive electrodes, and microfluidic channels, demonstrated reduced glial response three months after implantation.[107]

It is noteworthy that the polymer materials used in these examples still have Young's moduli orders of magnitude higher than that of the neural tissue, thus necessitating reliance on structural designs, such as ultrathin and macroporous electronics,[108, 109] to further improve the neural tissue interface, as will be discussed below. A recent demonstration of 'elastronics', which consists of a highly conductive soft hydrogel as the conductor and an elastic fluorinated photoresist as the insulating layer, successfully produced a bioelectronics neural implant with Young's modulus (10^4 – 10^5 Pa) similar to that of the neural tissue for the first time (Fig. 4A).[110] Owing to the tissue-like Young's moduli of the constituent materials, the soft elastronic arrays enabled ultralow voltage electrical stimulation of the mouse sciatic nerve. Furthermore, by employing tissue-like polymers with viscoplastic and self-healing properties, "morphing electronics" affords a reconfigurable and seamless neural interface that grows together with the sciatic nerve, thus allowing stable electrical stimulation during the fastest growth period in rats.[111]

Reduction of critical dimensions decreases bending stiffness

Besides replacement of harder materials with softer counterparts, it has also been demonstrated that reduction of critical dimensions can make nominally rigid materials mechanically compliant. For example, by varying the diameter and tip geometry of microwires, Obaid et al. demonstrated that a significantly tempered interfacial force, suggesting less tissue damage, upon insertion was measured for smaller-diameter microwires.[113] Similarly, microthread electrodes (MTEs) are ultrasmall composite electrodes, made with polymer-coated 7 μm diameter carbon fibers, which produce over 4 orders of magnitude increase in flexibility and over twice the fracture strength compared to silicon. Owing to these properties, Kozai et al. demonstrated chronic recordings in rats for up to 5 weeks with reduced chronic immune responses at implantation site.[48] Additionally, further reduction of feature sizes from micron-sized carbon fibers to 30 nm diameter multi-walled carbon nanotubes (CNTs) has been offered as a solution to improve the mechanical compliance and reduce the chronic immune responses of hard materials. By spinning CNTs into 10 μm diameter yarns, McCallum et al. demonstrated a 10-fold increase in conductivity and flexibility, compared to PtIr electrodes of the same diameter, as well as up to 16 weeks of recording stability in rat autonomic nerves.[114] Finally, a combination of softer materials with reduced feature sizes has led to the unprecedented tissue-like mechanical properties of NeuE which has demonstrated few to none chronic immune responses and seamless integration with neuronal circuitry (Fig. 4B).[63, 115, 116]

Strategies to address the challenges of delivery

However, there remains an intrinsic dilemma in creating neural interfaces that seamlessly integrate with the brain while minimizing the impact of brain penetration and insertion. Flexible and ultrathin neural probes conform to neural tissue and minimize chronic immune responses, yet these probes require a specialized insertion technique to avoid mechanical deformation during the implantation process, which is the prominent failure mode for these devices.[18, 26] Stiffeners and shape-memory polymers, which are inspired by stimulus-responsive materials found in biology, offer solutions for device implantation without buckling.[117, 118] By coating thin film polymer probes with bioresorbable PEG or silk fibroin, an otherwise flexible device may be inserted without crumpling.[119, 120] Freezing a highly flexible macroporous probe in liquid nitrogen has also been shown to demonstrate environment-induced softening, simply due to the thawing of ice without requiring an additional material-based coating.[121] In addition, by utilizing shape memory polymers, neural interfaces have been shown to soften *in vivo*, hosting a similar elastic modulus to neural tissue after insertion.[118] In an example inspired by twining plants, shape memory polymers have been employed to afford self-climbing of flexible electrodes onto peripheral nerves for *in vivo* stimulation and recording of nerve activity in rabbits.[122] Finally, by taking inspiration from the reversible hardening of sea cucumber dermis, bioinspired neural devices are capable of actively changing its stiffness via chemoresponsive and thermoresponsive composites, which can complement preexisting polymeric systems.[123]

Besides the approaches that involve a dynamic change of stiffness to facilitate insertion, mesh electronics are delivered precisely into the targeted brain regions via syringe-assisted injection.[124] Mesh electronics can be suspended in a biocompatible solution of phosphate buffered saline (PBS), loaded into a syringe needle, and delivered into the brain region of interest with stereotaxic syringe injection like pharmaceuticals.[124] Inspired by the shuttle device-assisted delivery of ultraflexible nanoelectronic probes, a scalable, automatable alternative to injection is a ‘sewing machine’-like rapid insertion, which guides devices into precise brain regions while evading essential vasculature to minimize the impact of insertion.[56, 65] Moreover, taking inspiration from the mechanisms behind the mosquito’s skin-piercing fascicles allows neural interfaces to be inserted with increased critical buckling force, and therefore greater precision free of crumpling (Fig. 4C).[112] In addition, distributing the load of flexible devices via microfluidic actuation offers an alternative to inserting neural interfaces that would otherwise buckle. By coupling a flexible microelectrode to a microfluidic channel, the fluid applies a viscous drag force to the microelectrode due to the velocity differential between the two, thus holding the device under tension in preparation for insertion.[62] Therefore, taking inspiration from biology, both within the brain and beyond, has the potential to improve the seamless integration of neural interfaces via improved mechanical compliance and optimized delivery methods to ultimately obtain a chronic interface for recording and modulating neural circuitry.

Bioinspired Topological Properties

In addition to revealing the intricate size and scale of neurons and neurites, the workings of Ramon y Cajal and Golgi also highlighted the elaborate connectivity between neurons and

the complex circuits they comprise.[125] Recent advances in electron microscopy and two-photon fluorescence microscopy have enabled the reconstruction of the three-dimensional (3D) network comprised of neurons and non-neuronal cells in the mouse brain with exceedingly convoluted connections and interactions.[126, 127] The brain is comprised of highly organized and interconnected networks of neurons and non-neuronal cells, such as astrocytes and microglia, which significantly contribute to neuronal function, that neural interfaces should ideally leave intact.[128] Despite knowledge of the underlying complexity of neural networks established in the late 19th century, early-stage bioelectronic neural interfaces were limited by available materials and techniques for fabrication.[11] Owing again to the technological advancements since the 1950's, 2D neural interfaces were developed as a direct result of planar microfabrication techniques.[129] As discussed in the section "Bioinspired Size and Morphology", these 2D structures allow for both a larger electrode packing density and the new capability of simultaneously measuring single-unit action potentials from multiple neurons, giving rise to knowledge of neural connectivity and circuitry.[130–132] By mimicking the structure of neurons and the topology of their corresponding circuitry in three dimensions, next-generation neural interfaces will provide an unprecedented perspective on the dynamics and evolution of neural function.

Neural interface topology pertains to both the global device shape and the local distribution of its electrodes and/or sensors. Generally, the global and local topologies of devices can be identical but are not necessarily so. For example, the tetrode is a one-dimensional (1D) bundle of four microwires, where four exposed electrodes lay on the end, thereby measuring signals from a small plane of neural tissue in 2D.[133] In contrast, the Utah-type MEA (Fig. 5, **top middle panel**) has its recording electrodes distributed laterally in 2D over a larger area (5×5 mm^2) on a planar silicon substrate.[20] This difference comes from distinct needs for neural signal measurement: the densely packed microwires in the tetrode are used for oversampled measurement and triangulation of action potentials from the same neurons,[134] while the Utah array is designed for sampling a larger volume of neural tissue with many neurons.[135] The historical evolution of neural interface topology, owing to materials discovery and modern processing techniques, is summarized to reveal a clear trend from lower-dimensional neural interfaces to 3D bioinspired topology (Fig. 1E).

Owing to the complex and dynamic structure of neural networks, we argue that there exist two principal opportunities for neural interface topology mimicry at different scales, which depend on the spatial distribution pattern of neurons.[25] On one hand, the retina hosts a curvilinear interface where the ganglion cells reside for visual processing and integration. Because of this, the optimal interface topology extends primarily to two dimensions (Fig. 5, **top middle column**). A key technology for retinal interfaces is the hexagonally packed 2D silicon-based photovoltaic array that can convert incoming light into electrical stimulus as retinal prosthetics.[53, 72, 136] On the other hand, the brain displays a high degree of interpenetration between the neuronal and glial networks in 3D;[126] therefore, an ideal bioelectronic neural interface implanted within the brain should be designed to afford a similar degree of interpenetration between the implanted electronic network and the endogenous neuronal and glial networks by leaving sufficient open space for interpenetration to occur. On a global scale, the cooperation of glial cells directs functional

connectivity and evolution of neuronal networks in the brain.[137, 138] Therefore, the device design should ensure an absence of or, at worst, minimal disturbance of the endogenous distribution of neurons and non-neuronal cells. Despite these design principles of an ideal neural probe, conventional probes necessarily exclude a solid volume of neural tissue permanently, thus not only prohibiting 3D interpenetration with the neuronal and glial networks but also disrupting the endogenous distribution of cells[139] and 3D diffusion of important molecular and macromolecular signaling species such as the inflammatory cytokines.[140] We note that both principal opportunities have driven the development from lower-dimensional neural interfaces to 3D bioinspired topology, and below we will discuss this trend in the topological evolution of neural probes for rigid and flexible bioelectronic neural interfaces, respectively.

Topological constraints for rigid neural interfaces

Rigid bioelectronic neural interfaces, which inherit the conventional designs and materials of neural electrophysiological probes, are progressing toward an increased density of electrodes, refined fabrication processes, and accommodating layouts of recording and stimulation sites in the topological evolution of neural probes. For example, while 1D devices were originally limited by available materials and processing techniques, such as Hubel's tungsten microwire (Fig. 5, **top left panel**),[11] modern devices have made a resurgence in low dimensions with a variety of fabrication and processing techniques. MTEs are created by coating 7 μm diameter 1D carbon fibers with polymers via chemical vapor deposition (CVD) and electrochemical deposition for the insulating layer and the recording site, respectively, resulting in an advanced 1D interface with reduced footprint and chronic immune responses as discussed above.[48] Similarly, CNTf microelectrodes utilize a clever fluidic microdrive insertion mechanism to deliver small carbon nanotube-based electrodes into the neural tissue, producing a 1D interface with neural tissue.[62] Additionally, the Behnke-Fried electrodes are comprised of bundled platinum-iridium microwires that spread out into the target brain region like a cone, thus maximizing the interfaced volume of neural tissue in the brain with a limited number of 1D microwire electrodes.[141] Meanwhile, multifunctional fibers have a topology similar to that of microwire electrode arrays such as the tetrode, where the device contains multiple electrodes on the end of a cylindrical structure to afford a 2D neural interface.[50, 142] Conventional 2D MEA configurations such as the Michigan and Utah type silicon arrays (Fig. 5, **top middle panel**) have also received improvements in the topology of neural interfacing. For example, the Neuropixels probe is built on the conventional 2D layout of a Michigan-type MEA with a much larger number of recording sites, benefiting from high resolution planar processing techniques (e.g., 130-nm CMOS technology) which allow recordings from a large population of neurons.[57] Similarly, Roukes et al. developed a 3D Michigan-type array comprising 16 silicon shanks in a 4×4 layout, affording up to 1024 electrodes in a 0.6 mm^3 footprint (Fig. 5, **top right panel**).[89] Lastly, the recent CMOS-integrated massively parallel microwire array integrates hundreds to thousands of fine micromachined microwires into a CMOS readout system for enhanced 3D interfacing with neural circuitry and readout technologies.[69]

Topological constraints for flexible neural interfaces

The popularization of flexible materials in neural interfaces allows for flexibility in device topology by reducing mechanical load and increasing device conformability to surrounding tissue.[143] The ultraflexible nanoelectronic probes (Fig. 2F, Fig. 3B, **ii**), for example, host a linear array of four or eight electrodes on a 1D flexible thread, and offer chronically stable recording of single-unit action potentials for four months (Fig. 5, **bottom left panel**).[56] Similarly, Neuralink offers 32-channel Michigan-style flexible threads that are implanted individually with a 'sewing machine'.[65] Comprising a 2D array of recording electrodes, NeuroGrid is a planar structure that, due to its flexibility, conforms to the irregularly curved three-dimensional structure of the cortical surface, offering measurement of both low-frequency ECoG signal and high-frequency single-unit action potentials from an extended area of the cortex (Fig. 5, **bottom middle panel**).[52, 144] Besides the ECoG-type interrogation of single-unit action potentials from the cortical surface, a flexible epicortical device, which is comprised of a distributed mesh of thin Si membrane and a polydimethylsiloxane (PDMS) substrate enables precise activation of limb movement via light-induced capacitive and Faradaic effect.[59, 145] Additionally, the ultraflexible and macroporous properties of mesh electronics allows for enhanced conformability to the curvilinear surface of the retina. Upon injection into the vitreous body of the eye, mesh electronics is capable of unfolding and coating the retinal surface to seamlessly interface with retinal ganglion cells (RGCs).[146] In addition to its ultraflexible properties, the macroporosity of mesh electronics allows for unimpeded light to interact with the retinal ganglion cells, preserving visual acuity and light perception during chronic *in vivo* retinal experiments.[146] This chronic 2D retinal interface enabled longitudinal study of RGCs after optic nerve crush, revealing dramatic differences in the physiological responses of distinct RGC types and their resilience to injury.[147] Further, by interfacing a fully organic device comprising a flexible silk substrate and layers of photoactive conjugated polymers, Maya-Vetencourt et al. demonstrated a fully-autonomous bioelectronic neural prosthesis that restores vision in both a rat model of degenerative blindness and of retinal dystrophy.[72, 136]

In addition, flexible low-dimensional devices introduce the opportunity for higher dimensional occupancy. Neurotassels incorporates flexible and independent 1D fibers that can span two- to three-dimensions upon insertion into the brain.[64] Similarly, NeuroRoots is a modular set of 1D electrodes that occupy a volume of neural tissue after being guided by a microwire (Fig. 5, **bottom right panel**).[61] Mesh electronics, by incorporating multiple ribbons of recording electrodes into a porous, 3D structure, enables neurite interpenetration[108] and prevents accumulation of inflammatory molecules.[121, 140] As a result, mesh electronics exhibits few to none chronic immune responses, evidenced by immunohistology, for up to one year post-injection.[115, 116] Likewise, NeuE is designed with a similar architecture, but with an increased porosity above 99% to further encourage neural circuitry interpenetration and NPC migration in 3D (Fig. 5, **bottom right panel**).[63]

By combining the advantages of flexible materials, advanced insertion techniques, and modern interfacing methodologies with higher-dimensional topologies mimicking those of the endogenous neural network, modern neural interfaces significantly reduce volume occupancy compared to traditional devices. Therefore, these topological design features

contribute to a much larger number of interfaced neurons, a significant reduction of nearby chronic immune responses and the maintenance of a close-to-native local environment of the neural tissue. We argue that bioinspired neural interface topologies, made possible by flexible materials and modern processing techniques, result in unprecedented chronic recording stability and high-dimensional conformability, and, ultimately, represent the next step towards seamless integration with endogenous neural circuitry.

Bioinspired Coatings and Functionalization

Neuroinflammation, the immune system's response to implanted neural interfaces within the central nervous system, is characterized by the accumulation of activated microglia and astrocytes at the implanted probe interface and exists in all stages of the device-brain interaction. A few weeks following implantation, activated microglia attach to the surface of the device and release proinflammatory and neurotoxic factors, eventually leading to neuronal death and device degradation.[28, 148–150] Around 6–8 weeks post-implantation, a glial scar, comprising microglia and astrocytes, will form an encapsulating layer around the implant, limiting axonal regeneration and preventing restoration of damage done to the blood-brain barrier (BBB) during implantation.[27, 149, 151] Because neuroinflammation comprises various cellular and chemical pathways, we argue that the local biochemical environment of the implanted bioelectronic neural interface can be modified via bioinspired surface coating and functionalization with a clear trend of surface-functionalized neural probes in recent years (Fig. 1F). These surface modification approaches will help suppress inflammation and promote neuronal growth, thus encouraging the regeneration of a native cellular environment at the neural tissue-implant interface.[27, 139, 152]

Anti-inflammatory coatings

Chronically stable neural interfaces have been developed by integrating anti-inflammatory coatings comprising endogenous molecules (Fig. 6, **right**). For example, alpha melanocyte-stimulating hormone (α-MSH) is an endogenous tridecapeptide, which is naturally produced by cells in the pituitary gland[153] and inhibits pro-inflammatory cytokines and neurotoxic nitric oxide production by microglia.[154] Additionally, α-MSH can directly mitigate microglial responses to foreign brain implants.[155] By depositing α-MSH onto Michigan-type silicon MEAs, a significantly attenuated glial response was found for at least four weeks post-implantation.[43] Similarly, dexamethasone is a synthetic glucocorticoid hormone used to treat many inflammatory responses via local delivery.[156] By either coating silicon-based Michigan arrays or retrofitting a flexible polyimide-based device for controlled release of dexamethasone, both an attenuated inflammatory response and a reduction of neuronal loss are achieved.[44, 157] Integrating minocycline, a broad synthetic tetracycline, to a bioelectronic neural interface can provide an additional pathway to the reduction of deleterious immune responses.[158] Combining a silicon oxide substrate, to mimic the surface of silicon-based MEAs (i.e. Utah and Michigan-type MEAs), with an engineered polymer film for sustained release of minocycline, resulted in a reduction of biomarkers associated with inflammation and retention of neuron viability within 46 days in comparison to an uncoated silicon oxide substrate.[158] Similarly, integrating a flexible microfluidic channel to silicon-parylene neural probes to administer minocycline into the local environment

produced a reduction in microglial reaction when compared to a plain silicon shank.[159] Another bioinspired approach to inhibit neuroinflammatory response is via targeting the receptor of a biomarker associated with the cascade of immune responses with the receptor's antagonist. IL-1 is a family of cytokines that is known for inducing scars and contributing to the pro-inflammatory response in the brain.[160] Coating silicon-based MEAs with IL1-receptor antagonist (IL1-ra), which blocks the receptor from the IL-1 cytokine molecules, produced significantly less glial scarring 4 weeks post-implantation compared to the non-coated MEA.[161]

Neuron-promoting coatings

In the 1950s, Levi-Montalcini and Cohen observed that chick embryos, after being injected with purified snake venom, exhibited an overgrowth of sensory and sympathetic ganglia and sympathetic nerve bundles.[162] By isolating nerve growth factor (NGF), a pro-growth and regenerative biological signaling molecule, Levi-Montalcini and Cohen produced the first of many neurotrophic factors, resulting in their joint Nobel Prize in Physiology or Medicine in 1986. Since then, numerous additional neurotrophic factors have been discovered and implemented *in vivo*, demonstrating both anti-inflammatory and pro-growth regeneration of neuronal cells.[100] The discovery of NGF and introduction to neurotrophic factors established an additional dimension to designing and implementing next-generation neural interfaces.[163, 164]

Neural regeneration-based long-term recording was first demonstrated *in vivo* in the late 1980's by implanting a 75 μm diameter Teflon-insulated gold wire inside a hollow glass tube containing a piece of sciatic nerve, which contained active NGF.[165] By inducing neurite growth, Kennedy et al. recorded single and multiple unit activity for up to twelve months in the motor cortex and demonstrated histological evidence for *in vivo* neurite growth. Additionally, extracellular matrix (ECM) materials can mitigate an inflammatory response due to their biocompatibility and biodegradability and, if incorporated in a scaffold-like framework, they have the potential to encourage neural regrowth.[166, 167] In addition to providing mechanical support, ECM materials encourage regrowth of endogenous tissue through their intrinsic properties (e.g., biochemical and mechanical cues). ECM materials have found significant application in stroke recovery models and have the potential to translate in other models of neural interface technologies.[168] For example, laminin is a key ECM regulator that plays crucial roles in cell adhesion, differentiation, migration and axonal pathfinding.[169] By coating eight bilayers of laminin on a silicon-based neural probe, there was a ~50% reduction in glial fibrillary acid protein (GFAP), an indicator for astrocytes, four weeks post-implantation.[170] Meanwhile, introducing a neural cell adhesion molecule may encourage neural regeneration while diminishing neuroinflammatory response (Fig. 6, **center**). L1, which is a transmembrane protein member of the L1 protein family, is a neuronal cell adhesion molecule expressed in the majority of neurons in the central nervous system (CNS), and is known to promote neuronal survival and migration.[46] By comparing L1-coated with non-coated four-shank Michigan-type MEAs, Cui et al. noted significantly less neural loss and a lower activation of microglia and astrocytes on the L1-coated device.[46] Inspired by the use of endogenous biological factors with the neurotrophic electrode and the mechanical and biochemical cues provided by the ECM, Lee et al. developed the Matrigel

coating, which is a biologically-derived hydrogel containing basement membrane proteins as well as growth factors.[171] By integrating Matrigel on a flexible parylene-C shank (optionally with the addition of dexamethasone), the authors demonstrated reduced electrical impedance during the first week and enhanced SNR at 14 weeks of recording relative to the uncoated shank.

While anti-inflammatory and neuron-promoting molecular coatings demonstrate the potential to curtail the chronic cascade of neuroinflammatory responses at the neural interface, most have been demonstrated on large and stiff devices (e.g., Michigan arrays). On one hand, this is advantageous as results can be interpreted to demonstrate some sort of "worst-case scenario". However, on the other hand, we envision that combining modern small and flexible neural interfaces with the advantages of anti-inflammatory coatings can realize enhanced chronic recording stability. We imagine that, by mimicking interfacial biochemical and mechanical properties, neural interfaces can 'trick' the immune system into accepting what might have normally been flagged as a foreign body. For example, bioresorbable silicon-based flexible electronics globally integrate bioresorbable materials to encourage conformal interfacing and complete dissolution to minimize chronic impacts (Fig. 2D).[55, 172, 173] By integrating a sheet of poly(lactic-co-glycolic) acid (PLGA) and silicon nanomembranes, the ECoG-like array serves as a bioinspired solution for minimally invasive integration with the cortical surface for up to 4–5 weeks.[55] Additionally, the incorporation of a PLGA fiber with a bioresorbable photodetector (comprised of a doped monocrystalline Si nanomembrane) and zinc electrodes yielded a bioresorbable spectrometer capable of measuring neural activity via calcium indicator transients, cerebral temperature, and cerebral oxygenation.[172]

Conclusion and Outlook

The fields of neuroengineering and neuroscience have intimately connected roots, yet their corresponding objectives have largely been independent. We argue that there exists a remarkable opportunity for these fields to engage and refine the means of interrogating and manipulating neural activity at an unprecedented resolution and scale through both a fundamental understanding of endogenous tissue, including its size, mechanical, topological, and biochemical properties, and the development of next-generation devices that allow for seamless integration with surrounding tissue (Fig. 7).

Because neural interface properties are fundamentally coupled in complex and seemingly mercurial ways, it is difficult, and even inappropriate, to argue the importance of one property above all others. Instead, to counsel the direction of this exceptionally interdisciplinary field, we highlight the impact that varying key properties, inspired by the brain and beyond, has on the device's ability to interface with endogenous neuronal circuitry. Therefore, we emphasize a modern trend of neural interface design (Fig. 1), where design principles are taken with an *a priori* knowledge of the properties of endogenous neural tissue and unlock unprecedented spatiotemporal resolution and scale. In particular, we reiterate key features of bioinspired neural interfaces:

- **Size and morphology:** The feature sizes and morphologies of neural interfaces afford the opportunity for greater spatial resolution, substantial multiplexing, and endogenous neural tissue acceptance.
- **Mechanical properties:** The device-brain interface improves as the bending stiffness of neural interfaces approaches that of adjacent neural tissue, thereby affording greater chronic recording stability.
- **Topological properties:** As the topology and interpenetration of neural interfaces increases, the opportunity for improved interfacing and neuroscience study in its native cellular environment is afforded.
- **Biochemical properties:** Coating or functionalizing neural interfaces with anti-inflammatory or neuron-promoting molecules influences the extent and magnitude of an inherent immune response to neural interface implantation.

With the progressing trend towards bioinspired bioelectronic neural interfaces, there exists a further opportunity for bidirectional information transfer. Stimulating neural devices have been demonstrated with significant clinical potential, such as the DBS electrode,[8] yet stimulating devices have not evolved to the same great extent as recording devices. We assert that, in addition to the potential for closed-loop feedback between neuroscience and neuroengineering advances (Fig. 7), there also exists a fortuitous opportunity for closed-loop bidirectional information transfer from the brain and the user, which could take the form beyond the conventional implantable electrodes and fiber optics. For example, significant strides have been made in developing wirelessly operating bioelectronic devices, evidenced by the recording capabilities of Neural Dust.[174] Additionally, by coupling a custom integrated circuit and energy storage capacitor to a piezoelectric transducer, StimDust affords low-power, wireless neural stimulation via ultrasonic power, with a minimal device volume footprint.[175] Similarly, the recent development of ‘sono-optogenetics’ from our lab has demonstrated a minimally invasive method of delivering nanoscopic light sources deep inside the brain via intravenous injection of mechanoluminescent nanoparticles and a brain-penetrant, ultrasound-based neural stimulation interface.[176] Besides the endogenous circulatory system in the body that has offered unique opportunities for delivery and formation of neural stimulation interfaces,[176, 177] there are plenty of bioinspired opportunities for establishing a bidirectional neural interface with the desired properties in Fig. 7. Bidirectional information transfer via a seamless neural interface has the potential to elucidate function and dysfunction of neural circuitry, as well as the ability to better inform more efficient, less invasive, and longer lasting neural therapies.

Beyond the ways in which the field can improve the front-end interface between the brain and the bioelectronic device, additional opportunities exist to refine back-end connections with recording and stimulation instruments. First, there is a need to improve the downstream connection between the bioelectronic neural interface and data acquisition and storage systems. This requirement is emphasized by understanding the trend towards larger electrode multiplexity (as seen in Fig. 1C). As electrode multiplexity of bioelectronic neural interfaces increases, standard connection methods (e.g., flat flexible cables) are no longer relevant and new, reliable systems are required. Recent efforts have tackled this looming

problem by taking inspiration from silicon-based technologies. For example, Neuropixels utilizes a customized CMOS-based connector and user-programmable switches to address 384 out of the 960 total electrodes simultaneously.[57] Taking a step further, a massively paralleled microwire array has been developed recently to mate to a variety of CMOS chips, allowing further opportunities for scalability and customizability.[69] The Argo system, taking a similar approach as the Neuropixels recording system and that of Obaid et al., affords the highest channel count of any *in vivo* bioelectronic neural interface with simultaneous recording of up to 65,536 channels at 32 kHz and 12-bit resolution.[73] By designing a custom, on-chip CMOS-based system capable of standard preprocessing (e.g., analog to digital conversion and amplification), the Argo system provides a high throughput end-to-end solution to high density recording.[73] Unlike spatially separated recording sites and data multiplexers, the implementation of on-shank CMOS multiplexing circuits on high electrode density probes (e.g. NeuroSeeker[178]) causes heat dissipation in the brain. The maximum power of these circuits must be curtailed to prevent excessive heating of tissue, limiting further increases in electrode multiplexity.[18, 179, 180] While placing all active electronics on the probe base can reduce tissue heating, this technique has its own limitation as it increases the size of the headstage.[18] Thus, further work is needed towards the optimal management of heat dissipation in high electrode density probes.

Furthermore, we envision the future of neural interfaces will surpass the conventional aim of achieving a physically seamless and high-throughput interface, additionally achieving a reliable and direct computational interface between the exogenous neural implants and the endogenous neural network that can process and analyze ultra-dense neural recording data efficiently.[181] Fortunately, this is already galvanizing with Neuralink's custom on-chip integrated circuit for real-time spike thresholding and wireless data transfer.[65] Going beyond this, we envision the potential to interface endogenous neuronal circuitry with neuromorphic devices.[182, 183] While neuromorphics were initially implemented to mimic desirable dynamics of neuronal computation, such as short-term and long-term potentiation involved in neuroplasticity, with silicon-based technology, these systems encompass much more. Now formed from inorganic and organic,[184] low-dimensional and layered (e.g., van der Waals) materials,[185] neuromorphic devices are envisioned to be efficient in memory computation via massive parallelism, capable of supervised and unsupervised learning, and strip the need for analog to digital (ADC) converters.[186] The integration of sensing elements into neuromorphic devices will enable the construction of artificial central and peripheral nervous systems, which could repair or augment existing neural tissue.[187] To unlock the great potential of chronic neuromorphic implants, this bio-influenced computational concept must be realized in bioinspired devices. By replacing energy demanding electronics with a system inspired by the tissue it measures, we envision a fundamental shift in what it means to listen to and mediate neural matter.

Progress and Potential Statement:

In the past decade, significant strides towards optimizing *in vivo* neural interfaces have been achieved with continuous materials advances. While modern materials discovery and fabrication techniques unlocked a fundamental avenue for remarkable progress of bioelectronic neural interfaces, a significant dimension impeding further progress emerges

from the lack of an *a priori* understanding of the properties of the neural tissue. By taking inspiration from the brain and biology, there exists a rich opportunity to develop bidirectional neural interfaces which seamlessly integrate with the endogenous tissue. This review focuses on an exciting new dimension by demonstrating how several principal properties of modern neurotechnology may optimize bidirectional transfer of information, based on fundamentally new structural, mechanical, topological, and biochemical design principles inspired by biology.

Acknowledgements

We thank R. Yin, Y. Chen, and T. Guo for helpful discussions. This work was supported by a National Institutes of Health (NIH) Pathway to Independence Award (National Institute on Aging 5R00AG056636-04) and Wu Tsai Neurosciences Institute of Stanford University.

References

1. Rivnay J, Wang H, Fenno L, Deisseroth K, and Malliaras GG (2017). Next-generation probes, particles, and proteins for neural interfacing. Sci. Adv 3, e1601649. [PubMed: 28630894]
2. Chen R, Canales A, and Anikeeva P (2017). Neural recording and modulation technologies. Nat. Rev. Mater 2, 16093. [PubMed: 31448131]
3. Patel SR, and Lieber CM (2019). Precision electronic medicine in the brain. Nat. Biotechnol 37, 1007–1012. [PubMed: 31477925]
4. Song E, Li J, Won SM, Bai W, and Rogers JA (2020). Materials for flexible bioelectronic systems as chronic neural interfaces. Nat. Mater 19, 590–603. [PubMed: 32461684]
5. Galvani L (1791). D viribus electricitatis in motu musculari: Commentarius. Bologna: Tip. Istituto delle Scienze, 1791; 58p.: 4 tavv. ft; in 4.; DCC. f. 70.
6. Fritsch G, and Hitzig E (2009). Electric excitability of the cerebrum (Über die elektrische Erregbarkeit des Grosshirns). Epilepsy Behav. 15, 123–130. [PubMed: 19457461]
7. Kringelbach ML, Jenkinson N, Owen SLF, and Aziz TZ (2007). Translational principles of deep brain stimulation. Nat. Rev. Neurosci 8, 623–635. [PubMed: 17637800]
8. Lozano AM, Lipsman N, Bergman H, Brown P, Chabardes S, Chang JW, Matthews K, McIntyre CC, Schlaepfer TE, Schulder M, et al. (2019). Deep brain stimulation: current challenges and future directions. Nat. Rev. Neurol 15, 148–160. [PubMed: 30683913]
9. Cogan SF (2008). Neural Stimulation and Recording Electrodes. Annu. Rev. Biomed. Eng 10, 275–309. [PubMed: 18429704]
10. Cagnan H, Denison T, McIntyre C, and Brown P (2019). Emerging technologies for improved deep brain stimulation. Nat. Biotechnol 37, 1024–1033. [PubMed: 31477926]
11. Hubel DH (1957). Tungsten microelectrode for recording from single units. Science 125, 549–550. [PubMed: 17793797]
12. Patel SR, Sheth SA, Martinez-Rubio C, Mian MK, Asaad WF, Gerrard JL, Kwon C-S, Dougherty DD, Flaherty AW, Greenberg BD, et al. (2013). Studying task-related activity of individual neurons in the human brain. Nat. Protoc 8, 949–957. [PubMed: 23598445]
13. Neher E, and Sakmann B (1976). Single-channel currents recorded from membrane of denervated frog muscle fibres. Nature 260, 799–802. [PubMed: 1083489]
14. Sakmann B, and Neher E (1984). Patch Clamp Techniques for Studying Ionic Channels in Excitable Membranes. Annu. Rev. Physiol 46, 455–472. [PubMed: 6143532]
15. Hamill OP, and McBride DW (1997). Induced Membrane Hypo/Hyper-Mechanosensitivity: A Limitation of Patch-Clamp Recording. Annu. Rev. Physiol 59, 621–631. [PubMed: 9074780]
16. Henze DA, Borhegyi Z, Csicsvari J, Mamiya A, Harris KD, and Buzsáki G (2000). Intracellular Features Predicted by Extracellular Recordings in the Hippocampus In Vivo. J. Neurophysiol 84, 390–400. [PubMed: 10899213]

17. Hunt DL, Lai C, Smith RD, Lee AK, Harris TD, and Barbic M (2019). Multimodal in vivo brain electrophysiology with integrated glass microelectrodes. Nat. Biomed. Eng 3, 741–753. [PubMed: 30936430]
18. Hong G, and Lieber CM (2019). Novel electrode technologies for neural recordings. Nat. Rev. Neurosci 20, 330–345. [PubMed: 30833706]
19. Wise KD, Angell JB, and Starr A (1970). An Integrated-Circuit Approach to Extracellular Microelectrodes. IEEE Trans. Biomed. Eng BME-17, 238–247.
20. Campbell PK, Jones KE, and Normann RA (1990). A 100 electrode intracortical array: Structural variability. Biomed. Sci. Instrum 26, 161–165. [PubMed: 2334761]
21. Drake KL, Wise KD, Farraye J, Anderson DJ, and BeMent SL (1988). Performance of Planar Multisite Microprobes in Recording Extracellular Single-Unit Intracortical Activity. IEEE Trans. Biomed. Eng 35, 719–732. [PubMed: 3169824]
22. Campbell PK, Jones KE, Huber RJ, Horch KW, and Normann RA (1991). A Silicon-Based, Three-Dimensional Neural Interface: Manufacturing Processes for an Intracortical Electrode Array. IEEE Trans. Biomed. Eng 38, 758–768. [PubMed: 1937509]
23. Shoffstall AJ, and Capadona JR (2018). Bioinspired materials and systems for neural interfacing. In Current Opinion in Biomedical Engineering, Volume 6 (Elsevier Ltd), pp. 110–119.
24. Li H, Wang J, and Fang Y (2020). Bioinspired flexible electronics for seamless neural interfacing and chronic recording. Nanoscale Adv, DOI: 10.1039/d1030na00323a.
25. Hong G, Viveros RD, Zwang TJ, Yang X, and Lieber CM (2018). Tissue-like Neural Probes for Understanding and Modulating the Brain. Biochemistry 57, 3995–4004. [PubMed: 29529359]
26. Obidin N, Tasnim F, and Dagdeviren C (2020). The Future of Neuroimplantable Devices: A Materials Science and Regulatory Perspective. Adv. Mater 32, 1901482.
27. Polikov VS, Tresco PA, and Reichert WM (2005). Response of brain tissue to chronically implanted neural electrodes. J. Neurosci. Methods 148, DOI: 10.1016/j.jneumeth.2005.1008.1015.
28. Salatino JW, Ludwig KA, Kozai TDY, and Purcell EK (2017). Glial responses to implanted electrodes in the brain. Nat. Biomed. Eng 1, 862–877. [PubMed: 30505625]
29. Cicchetti F, and Barker RA (2014). The glial response to intracerebrally delivered therapies for neurodegenerative disorders: Is this a critical issue? Front. Pharmacol 5, 139. [PubMed: 25071571]
30. Acarón Ledesma H, Li X, Carvalho-de-Souza JL, Wei W, Bezanilla F, and Tian B (2019). An atlas of nano-enabled neural interfaces. Nat. Nanotechnol 14, 645–657. [PubMed: 31270446]
31. Frank JA, Antonini M-J, and Anikeeva P (2019). Next-generation interfaces for studying neural function. Nat. Biotechnol 37, 1013–1023. [PubMed: 31406326]
32. Oyster CW, Takahashi ES, and Hurst DC (1982). Analysis of neuronal soma size distributions. J. Neurosci. Methods 6, 311–326. [PubMed: 7154713]
33. Liewald D, Miller R, Logothetis N, Wagner HJ, and Schüz A (2014). Distribution of axon diameters in cortical white matter: an electron-microscopic study on three human brains and a macaque. Biol. Cybern 108, 541–557. [PubMed: 25142940]
34. Sterling P, and Laughlin S (2015). Principles of Neural Design, (MIT Press).
35. Herculano-Houzel S, Mota B, and Lent R (2006). Cellular scaling rules for rodent brains. Proc. Natl. Acad. Sci. USA 103, 12138–12143. [PubMed: 16880386]
36. Hinsch K, and Zupanc GKH (2007). Generation and long-term persistence of new neurons in the adult zebrafish brain: A quantitative analysis. Neuroscience 146, 679–696. [PubMed: 17395385]
37. Lagercrantz H, Hanson MA, Ment LR, and Peebles DM eds. (2010). The Newborn Brain: Neuroscience and Clinical Applications, 2nd Edition (Cambridge University Press).
38. Cash D, and Carew TJ (1989). A quantitative analysis of the development of the central nervous system in juvenile Aplysia californica. J. Neurobiol 20, 25–47. [PubMed: 2921607]
39. Bode H, Berking S, David CN, Gierer A, Schaller H, and Trenkner R (1973). Quantitative analysis of cell types during growth and morphogenesis in Hydra. Wilhelm Roux Arch. Entwickl. Mech. Org 171, 269–285. [PubMed: 28304608]
40. Bechtereva NP, Bondartchuk AN, and Smirnov VM (1972). Therapeutic electrostimulations of the deep brain strucutres. Vopr. Neirokhir 1, 7–12.

41. Recce ML, and O'Keefe J (1989). The tetrode: a new technique for multi-unit extracellular recording. Soc. Neurosci. Abstr 15, 1250.
42. Rousche PJ, Pellinen DS, Pivin DP, Williams JC, Vetter RJ, and Kipke DR (2001). Flexible polyimide-based intracortical electrode arrays with bioactive capability. IEEE Trans. Biomed. Eng 48, 361–371. [PubMed: 11327505]
43. He W, McConnell GC, Schneider TM, and Bellamkonda RV (2007). A novel anti-inflammatory surface for neural electrodes. Adv. Mater 19, 3529–3533.
44. Zhong Y, and Bellamkonda RV (2007). Dexamethasone-coated neural probes elicit attenuated inflammatory response and neuronal loss compared to uncoated neural probes. Brain Res. 1148, 15–27. [PubMed: 17376408]
45. Bartels J, Andreasen D, Ehirim P, Mao H, Seibert S, Wright EJ, and Kennedy P (2008). Neurotrophic electrode: Method of assembly and implantation into human motor speech cortex. J. Neurosci. Methods 174, 168–176. [PubMed: 18672003]
46. Azemi E, Lagenaur CF, and Cui XT (2011). The surface immobilization of the neural adhesion molecule L1 on neural probes and its effect on neuronal density and gliosis at the probe/tissue interface. Biomaterials 32, 681–692. [PubMed: 20933270]
47. Wu F, Im M, and Yoon E (2011). A flexible fish-bone-shaped neural probe strengthened by biodegradable silk coating for enhanced biocompatibility. In 16th International Solid-State Sensors, Actuators and Microsystems Conference (IEEE), pp. 966–969.
48. Kozai TDY, Langhals NB, Patel PR, Deng X, Zhang H, Smith KL, Lahann J, Kotov NA, and Kipke DR (2012). Ultrasmall implantable composite microelectrodes with bioactive surfaces for chronic neural interfaces. Nat. Mater 11, 1065–1073. [PubMed: 23142839]
49. Fu TM, Duan X, Jiang Z, Dai X, Xie P, Cheng Z, and Lieber CM (2014). Sub-10-nm intracellular bioelectronic probes from nanowire-nanotube heterostructures. Proc. Natl. Acad. Sci. USA 111, 1259–1264. [PubMed: 24474745]
50. Canales A, Jia X, Froriep UP, Koppes RA, Tringides CM, Selvidge J, Lu C, Hou C, Wei L, Fink Y, et al. (2015). Multifunctional fibers for simultaneous optical, electrical and chemical interrogation of neural circuits in vivo. Nat. Biotechnol 33, 277–284. [PubMed: 25599177]
51. Minev IR, Musienko P, Hirsch A, Barraud Q, Wenger N, Moraud EM, Gandar J, Capogrosso M, Milekovic T, Asboth L, et al. (2015). Electronic dura mater for long-term multimodal neural interfaces. Science 347, 159–163. [PubMed: 25574019]
52. Khodagholy D, Gelinas JN, Thesen T, Doyle W, Devinsky O, Malliaras GG, and Buzsáki G (2015). NeuroGrid: Recording action potentials from the surface of the brain. Nat. Neurosci 18, 310–315. [PubMed: 25531570]
53. Lorach H, Goetz G, Smith R, Lei X, Mandel Y, Kamins T, Mathieson K, Huie P, Harris J, Sher A, et al. (2015). Photovoltaic restoration of sight with high visual acuity. Nat. Med 21, 476–482. [PubMed: 25915832]
54. Oxley TJ, Opie NL, John SE, Rind GS, Ronayne SM, Wheeler TL, Judy JW, McDonald AJ, Dornom A, Lovell TJH, et al. (2016). Minimally invasive endovascular stent-electrode array for high-fidelity, chronic recordings of cortical neural activity. Nat. Biotechnol 34, 320–327. [PubMed: 26854476]
55. Yu KJ, Kuzum D, Hwang SW, Kim BH, Juul H, Kim NH, Won SM, Chiang K, Trumpis M, Richardson AG, et al. (2016). Bioresorbable silicon electronics for transient spatiotemporal mapping of electrical activity from the cerebral cortex. Nat. Mater 15, 782–791. [PubMed: 27088236]
56. Luan L, Wei X, Zhao Z, Siegel JJ, Potnis O, Tuppen CA, Lin S, Kazmi S, Fowler RA, Holloway S, et al. (2017). Ultraflexible nanoelectronic probes form reliable, glial scar–free neural integration. Sci. Adv 3, e1601966. [PubMed: 28246640]
57. Jun JJ, Steinmetz NA, Siegle JH, Denman DJ, Bauza M, Barbarits B, Lee AK, Anastassiou CA, Andrei A, Aydin Ç, et al. (2017). Fully integrated silicon probes for high-density recording of neural activity. Nature 551, 232–236. [PubMed: 29120427]
58. Fu TM, Hong G, Viveros RD, Zhou T, and Lieber CM (2017). Highly scalable multichannel mesh electronics for stable chronic brain electrophysiology. Proc. Natl. Acad. Sci. USA 114, E10046–E10055. [PubMed: 29109247]

59. Jiang Y, Li X, Liu B, Yi J, Fang Y, Shi F, Gao X, Sudzilovsky E, Parameswaran R, Koehler K, et al. (2018). Rational design of silicon structures for optically controlled multiscale biointerfaces. Nat. Biomed. Eng 2, 508–521. [PubMed: 30906646]
60. Tang J, Qin N, Chong Y, Diao Y, Yiliguma, Wang Z, Xue T, Jiang M, Zhang J, and Zheng G (2018). Nanowire arrays restore vision in blind mice. Nat. Commun 9, 786. [PubMed: 29511183]
61. Ferro MD, Proctor CM, Gonzalez A, Zhao E, Slezia A, Pas J, Dijk G, Donahue MJ, Williamson A, Malliaras GG, et al. (2018). NeuroRoots, a bio-inspired, seamless Brain Machine Interface device for long-term recording. bioRxiv, 460949.
62. Vitale F, Vercosa DG, Rodriguez AV, Pamulapati SS, Seibt F, Lewis E, Yan JS, Badhiwala K, Adnan M, Royer-Carfagni G, et al. (2018). Fluidic Microactuation of Flexible Electrodes for Neural Recording. Nano Lett. 18, 326–335. [PubMed: 29220192]
63. Yang X, Zhou T, Zwang TJ, Hong G, Zhao Y, Viveros RD, Fu TM, Gao T, and Lieber CM (2019). Bioinspired neuron-like electronics. Nat. Mater 18, 510–517. [PubMed: 30804509]
64. Guan S, Wang J, Gu X, Zhao Y, Hou R, Fan H, Zou L, Gao L, Du M, Li C, et al. (2019). Elastocapillary self-assembled neurotassels for stable neural activity recordings. Sci. Adv 5, eaav2842. [PubMed: 30944856]
65. Musk E (2019). An Integrated Brain-Machine Interface Platform With Thousands of Channels. J. Med. Internet. Res 21, e16194. [PubMed: 31642810]
66. Chung JE, Joo HR, Fan JL, Liu DF, Barnett AH, Chen S, Geaghan-Breiner C, Karlsson MP, Karlsson M, Lee KY, et al. (2019). High-Density, Long-Lasting, and Multi-region Electrophysiological Recordings Using Polymer Electrode Arrays. Neuron 101, 21–31.e25. [PubMed: 30502044]
67. Jayant K, Wenzel M, Bando Y, Hamm JP, Mandriota N, Rabinowitz JH, Plante IJL, Owen JS, Sahin O, Shepard KL, et al. (2019). Flexible Nanopipettes for Minimally Invasive Intracellular Electrophysiology In Vivo. Cell Rep. 26, 266–278. [PubMed: 30605681]
68. Zhao Y, You SS, Zhang A, Lee J-H, Huang J, and Lieber CM (2019). Scalable ultrasmall three-dimensional nanowire transistor probes for intracellular recording. Nat. Nanotechnol 14, 783–790. [PubMed: 31263191]
69. Obaid A, Hanna ME, Wu YW, Kollo M, Racz R, Angle MR, Müller J, Brackbill N, Wray W, Franke F, et al. (2020). Massively parallel microwire arrays integrated with CMOS chips for neural recording. Sci. Adv 6, eaay2789. [PubMed: 32219158]
70. Chiang C-H, Won SM, Orsborn AL, Yu KJ, Trumpis M, Bent B, Wang C, Xue Y, Min S, Woods V, et al. (2020). Development of a neural interface for high-definition, long-term recording in rodents and nonhuman primates. Sci. Transl. Med 12, eaay4682. [PubMed: 32269166]
71. Cea C, Spyropoulos GD, Jastrzebska-Perfect P, Ferrero JJ, Gelinas JN, and Khodagholy D (2020). Enhancement-mode ion-based transistor as a comprehensive interface and real-time processing unit for in vivo electrophysiology. Nat. Mater 19, 679–686. [PubMed: 32203456]
72. Maya-Vetencourt JF, Manfredi G, Mete M, Colombo E, Bramini M, Di Marco S, Shmal D, Mantero G, Dipalo M, Rocchi A, et al. (2020). Subretinally injected semiconducting polymer nanoparticles rescue vision in a rat model of retinal dystrophy. Nat. Nanotechnol, DOI: 10.1038/s41565-41020-40696-41563.
73. Sahasrabuddhe K, Khan AA, Singh AP, Stern TM, Ng Y, Tadić A, Orel P, LaReau C, Pouzzner D, Nishimura K, et al. (2020). The Argo: A 65,536 channel recording system for high density neural recording in vivo. bioRxiv, 2020.2007.2017.209403.
74. Ramón y Cajal S, DeFelipe J, Jones EG, and May RM (1991). Cajal's degeneration and regeneration of the nervous system, (Oxford University Press).
75. Savtchenko LP, and Rusakov DA (2007). The optimal height of the synaptic cleft. Proc. Natl. Acad. Sci. USA 104, 1823–1828. [PubMed: 17261811]
76. Buzsáki G, Anastassiou CA, and Koch C (2012). The origin of extracellular fields and currents - EEG, ECoG, LFP and spikes. Nat. Rev. Neurosci 13, 407–420. [PubMed: 22595786]
77. Hodgkin AL, and Huxley AF (1939). Action potentials recorded from inside a nerve fibre. Nature 144, 710–711.

78. Anselme K, Davidson P, Popa AM, Giazzon M, Liley M, and Ploux L (2010). The interaction of cells and bacteria with surfaces structured at the nanometre scale. Acta Biomater. 6, 3824–3846. [PubMed: 20371386]

79. Manfrinato VR, Zhang L, Su D, Duan H, Hobbs RG, Stach EA, and Berggren KK (2013). Resolution Limits of Electron-Beam Lithography toward the Atomic Scale. Nano Lett. 13, 1555–1558. [PubMed: 23488936]

80. Piljek P, Keran Z, and Math M (2014). Micromachining–review of literature from 1980 to 2010. Interdiscip. Description Complex Syst 12, 1–27.

81. Viswam V, Obien MEJ, Franke F, Frey U, and Hierlemann A (2019). Optimal Electrode Size for Multi-Scale Extracellular-Potential Recording From Neuronal Assemblies. Front. Neurosci 13, 385. [PubMed: 31105515]

82. (2018). Bottom-up biology. Nature 563, 171. [PubMed: 30405231]

83. Tian B, Xie P, Kempa TJ, Bell DC, and Lieber CM (2009). Single-crystalline kinked semiconductor nanowire superstructures. Nat. Nanotechnol 4, 824–829. [PubMed: 19893521]

84. Tian B, Cohen-Karni T, Qing Q, Duan X, Xie P, and Lieber CM (2010). Three-Dimensional, Flexible Nanoscale Field-Effect Transistors as Localized Bioprobes. Science 329, 830–834. [PubMed: 20705858]

85. Qing Q, Jiang Z, Xu L, Gao R, Mai L, and Lieber CM (2014). Free-standing kinked nanowire transistor probes for targeted intracellular recording in three dimensions. Nat. Nanotechnol 9, 142–147. [PubMed: 24336402]

86. Zhang X (2019). Nanowires Pin Neurons: a Nano “Moon Landing”. Matter 1, 560–562.

87. Iqbal P, Preece JA, and Mendes PM (2012). Nanotechnology: The “Top-Down” and “Bottom-Up” Approaches In Supramol. Chem, Gale PA and Steed JW, eds. (John Wiley and Sons).

88. Scholvin J, Kinney JP, Bernstein JG, Moore-Kochlacs C, Kopell N, Fonstad CG, and Boyden ES (2016). Close-Packed Silicon Microelectrodes for Scalable Spatially Oversampled Neural Recording. IEEE Trans. Biomed. Eng 63, 120–130. [PubMed: 26699649]

89. Rios G, Lubenov EV, Chi D, Roukes ML, and Siapas AG (2016). Nanofabricated Neural Probes for Dense 3-D Recordings of Brain Activity. Nano Lett. 16, 6857–6862. [PubMed: 27766885]

90. Broers AN, Hoole Andrew ACF, and Ryan JM (1996). Electron beam lithography - Resolution limits. Microelectron. Eng 32, 131–142.

91. Mora Lopez C, Putzeys J, Raducanu BC, Ballini M, Wang S, Andrei A, Rochus V, Vandebriel R, Severi S, Van Hoof C, et al. (2017). A Neural Probe with Up to 966 Electrodes and Up to 384 Configurable Channels in 0.13 μm SOI CMOS. IEEE Trans. Biomed. Circuits Syst 11, 510–522. [PubMed: 28422663]

92. Cohen-Karni T, Casanova D, Cahoon JF, Qing Q, Bell DC, and Lieber CM (2012). Synthetically encoded ultrashort-channel nanowire transistors for fast, pointlike cellular signal detection. Nano Lett. 12, 2639–2644. [PubMed: 22468846]

93. Zhang A, and Lieber CM (2016). Nano-Bioelectronics. Chem. Rev 116, 215–257. [PubMed: 26691648]

94. Wellman SM, Li L, Yaxiaer Y, McNamara I, and Kozai TDY (2019). Revealing Spatial and Temporal Patterns of Cell Death, Glial Proliferation, and Blood-Brain Barrier Dysfunction Around Implanted Intracortical Neural Interfaces. Front. Neurosci 13, 493. [PubMed: 31191216]

95. Wellman SM, and Kozai TDY (2018). In vivo spatiotemporal dynamics of NG2 glia activity caused by neural electrode implantation. Biomaterials 164, 121–133. [PubMed: 29501892]

96. Lee S, Leach MK, Redmond SA, Chong SYC, Mellon SH, Tuck SJ, Feng ZQ, Corey JM, and Chan JR (2012). A culture system to study oligodendrocyte myelination processes using engineered nanofibers. Nat. Methods 9, 917–922. [PubMed: 22796663]

97. James R, Kim Y, Hockberger PE, and Szele FG (2011). Subventricular zone cell migration: Lessons from quantitative two-photon microscopy. Front. Neurosci 5, 30. [PubMed: 21472025]

98. Wellman SM, Eles JR, Ludwig KA, Seymour JP, Michelson NJ, McFadden WE, Vazquez AL, and Kozai TDY (2018). A Materials Roadmap to Functional Neural Interface Design. Adv. Funct. Mater 28, 1701269. [PubMed: 29805350]

99. Kozai TDY, Marzullo TC, Hooi F, Langhals NB, Majewska AK, Brown EB, and Kipke DR (2010). Reduction of neurovascular damage resulting from microelectrode insertion into the cerebral cortex using in vivo two-photon mapping. J. Neural Eng 7, 046011. [PubMed: 20644246]
100. Jorfi M, Skousen JL, Weder C, and Capadona JR (2015). Progress towards biocompatible intracortical microelectrodes for neural interfacing applications. J. Neural Eng 12, 011001. [PubMed: 25460808]
101. Lacour SP, Courtine G, and Guck J (2016). Materials and technologies for soft implantable neuroprostheses. Nat. Rev. Mater 1, 16063.
102. Rall W (2011). Core Conductor Theory and Cable Properties of Neurons In Comprehensive Physiology, Terjung R, ed. (American Cancer Society), pp. 39–97.
103. Hibbeler RC (2011). Mechanics of Materials, 8th Edition, (Pearson).
104. Subbaroyan J, Martin DC, and Kipke DR (2005). A finite-element model of the mechanical effects of implantable microelectrodes in the cerebral cortex. J. Neural Eng 2, 103–113. [PubMed: 16317234]
105. Torrente-Rodríguez RM, Tu J, Yang Y, Min J, Wang M, Song Y, Yu Y, Xu C, Ye C, IsHak WW, et al. (2020). Investigation of Cortisol Dynamics in Human Sweat Using a Graphene-Based Wireless mHealth System. Matter 2, 921–937. [PubMed: 32266329]
106. Yang Y, Song Y, Bo X, Min J, Pak OS, Zhu L, Wang M, Tu J, Kogan A, Zhang H, et al. (2020). A laser-engraved wearable sensor for sensitive detection of uric acid and tyrosine in sweat. Nat. Biotechnol 38, 217–224. [PubMed: 31768044]
107. Park S, Guo Y, Jia X, Choe HK, Grena B, Kang J, Park J, Lu C, Canales A, Chen R, et al. (2017). One-step optogenetics with multifunctional flexible polymer fibers. Nat. Neurosci 20, 612–619. [PubMed: 28218915]
108. Liu J, Fu TM, Cheng Z, Hong G, Zhou T, Jin L, Duvvuri M, Jiang Z, Kruskal P, Xie C, et al. (2015). Syringe-injectable electronics. Nat. Nanotechnol 10, 629–635. [PubMed: 26053995]
109. Hong G, Yang X, Zhou T, and Lieber CM (2018). Mesh electronics: a new paradigm for tissue-like brain probes. Curr. Opin. Neurobiol 50, 33–41. [PubMed: 29202327]
110. Liu Y, Liu J, Chen S, Lei T, Kim Y, Niu S, Wang H, Wang X, Foudeh AM, Tok JBH, et al. (2019). Soft and elastic hydrogel-based microelectronics for localized low-voltage neuromodulation. Nat. Biomed. Eng 3, 58–68. [PubMed: 30932073]
111. Liu Y, Li J, Song S, Kang J, Tsao Y, Chen S, Mottini V, McConnell K, Xu W, Zheng Y-Q, et al. (2020). Morphing electronics enable neuromodulation in growing tissue. Nat. Biotechnol, DOI: 10.1038/s41587-41020-40495-41582.
112. Shoffstall AJ, Srinivasan S, Willis M, Stiller AM, Ecker M, Voit WE, Pancrazio JJ, and Capadona JR (2018). A Mosquito Inspired Strategy to Implant Microprobes into the Brain. Sci. Rep 8, 122. [PubMed: 29317748]
113. Obaid A, Wu Y-W, Hanna M, Nix W, Ding J, and Melosh N (2018). Ultra-sensitive measurement of brain penetration with microscale probes for brain machine interface considerations. bioRxiv, 454520.
114. McCallum GA, Sui X, Qiu C, Marmerstein J, Zheng Y, Eggers TE, Hu C, Dai L, and Durand DM (2017). Chronic interfacing with the autonomic nervous system using carbon nanotube (CNT) yarn electrodes. Sci. Rep 7, 11723. [PubMed: 28916761]
115. Fu TM, Hong G, Zhou T, Schuhmann TG, Viveros RD, and Lieber CM (2016). Stable long-term chronic brain mapping at the single-neuron level. Nat. Methods 13, 875–882. [PubMed: 27571550]
116. Zhou T, Hong G, Fu TM, Yang X, Schuhmann TG, Viveros RD, and Lieber CM (2017). Syringe-injectable mesh electronics integrate seamlessly with minimal chronic immune response in the brain. Proc. Natl. Acad. Sci. USA 114, 5894–5899. [PubMed: 28533392]
117. Lewitus D, Smith KL, Shain W, and Kohn J (2011). Ultrafast resorbing polymers for use as carriers for cortical neural probes. Acta Biomater. 7, 2483–2491. [PubMed: 21345383]
118. Ware T, Simon D, Arreaga-Salas DE, Reeder J, Rennaker R, Keefer EW, and Voit W (2012). Fabrication of responsive, softening neural interfaces. Adv. Funct. Mater 22, 3470–3479.

119. Felix SH, Shah KG, Tolosa VM, Sheth HJ, Tooker AC, Delima TL, Jadhav SP, Frank LM, and Pannu SS (2013). Insertion of flexible neural probes using rigid stiffeners attached with biodissolvable adhesive. J. Vis. Exp, e50609. [PubMed: 24121443]
120. Kim T. i., McCall JG, Jung YH, Huang X, Siuda ER, Li Y, Song J, Song YM, Pao HA, Kim R-H, et al. (2013). Injectable, Cellular-Scale Optoelectronics with Applications for Wireless Optogenetics. Science 340, 211. [PubMed: 23580530]
121. Xie C, Liu J, Fu TM, Dai X, Zhou W, and Lieber CM (2015). Three-dimensional macroporous nanoelectronic networks as minimally invasive brain probes. Nat. Mater 14, 1286–1292. [PubMed: 26436341]
122. Zhang Y, Zheng N, Cao Y, Wang F, Wang P, Ma Y, Lu B, Hou G, Fang Z, Liang Z, et al. (2019). Climbing-inspired twining electrodes using shape memory for peripheral nerve stimulation and recording. Sci. Adv 5, eaaw1066. [PubMed: 31086809]
123. Capadona JR, Shanmuganathan K, Tyler DJ, Rowan SJ, and Weder C (2008). Stimuli-responsive polymer nanocomposites inspired by the sea cucumber dermis. Science 319, 1370–1374. [PubMed: 18323449]
124. Hong G, Fu TM, Zhou T, Schuhmann TG, Huang J, and Lieber CM (2015). Syringe Injectable Electronics: Precise Targeted Delivery with Quantitative Input/Output Connectivity. Nano Lett. 15, 6979–6984. [PubMed: 26317328]
125. Swanson LW, Newman E, Araque A, and Dubinsky JM (2017). The Beautiful Brain: The Drawings of Santiago Ramon y Cajal, (Abrams).
126. Kasthuri N, Hayworth KJ, Berger DR, Schalek RL, Conchello JA, Knowles-Barley S, Lee D, Vázquez-Reina A, Kaynig V, Jones TR, et al. (2015). Saturated Reconstruction of a Volume of Neocortex. Cell 162, 648–661. [PubMed: 26232230]
127. Winnubst J, Bas E, Ferreira TA, Wu Z, Economo MN, Edson P, Arthur BJ, Bruns C, Rokicki K, Schauder D, et al. (2019). Reconstruction of 1,000 Projection Neurons Reveals New Cell Types and Organization of Long-Range Connectivity in the Mouse Brain. Cell 179, 268–281.e213. [PubMed: 31495573]
128. Allen NJ, and Barres BA (2009). Glia - more than just brain glue. Nature 457, 675–677. [PubMed: 19194443]
129. (2018). 60 Years of Integrated Circuits. Nat. Electron 1, 483.
130. Rousche PJ, and Normann RA (1998). Chronic recording capability of the Utah Intracortical Electrode array in cat sensory cortex. J. Neurosci. Methods 82, DOI: 10.1016/S0165-0270(1098)00031-00034.
131. Fujisawa S, Amarasingham A, Harrison MT, and Buzsáki G (2008). Behavior-dependent short-term assembly dynamics in the medial prefrontal cortex. Nat. Neurosci 11, 823–833. [PubMed: 18516033]
132. Barthó P, Hirase H, Monconduit L, Zugaro M, Harris KD, and Buzsáki G (2004). Characterization of neocortical principal cells and interneurons by network interactions and extracellular features. J. Neurophysiol 92, 600–608. [PubMed: 15056678]
133. Jog MS, Connolly CI, Kubota Y, Iyengar DR, Garrido L, Harlan R, and Graybiel AM (2002). Tetrode technology: Advances in implantable hardware, neuroimaging, and data analysis techniques. J. Neurosci. Methods 117, 141–152. [PubMed: 12100979]
134. McNaughton BL, O'Keefe J, and Barnes CA (1983). The stereotrode: A new technique for simultaneous isolation of several single units in the central nervous system from multiple unit records. J. Neurosci. Methods 8, 391–397. [PubMed: 6621101]
135. Gilja V, Pandarinath C, Blabe CH, Nuyujukian P, Simeral JD, Sarma AA, Sorice BL, Perge JA, Jarosiewicz B, Hochberg LR, et al. (2015). Clinical translation of a high-performance neural prosthesis. Nat. Med 21, 1142–1145. [PubMed: 26413781]
136. Maya-Vetencourt JF, Ghezzi D, Antognazza MR, Colombo E, Mete M, Feyen P, Desii A, Buschiazzo A, Di Paolo M, Di Marco S, et al. (2017). A fully organic retinal prosthesis restores vision in a rat model of degenerative blindness. Nat. Mater 16, 681–689. [PubMed: 28250420]
137. Eroglu C, and Barres BA (2010). Regulation of synaptic connectivity by glia. Nature 468, 223–231. [PubMed: 21068831]

138. Clarke LE, and Barres BA (2013). Emerging roles of astrocytes in neural circuit development. Nat. Rev. Neurosci 14, 311–321. [PubMed: 23595014]
139. Biran R, Martin DC, and Tresco PA (2005). Neuronal cell loss accompanies the brain tissue response to chronically implanted silicon microelectrode arrays. Exp. Neurol 195, 115–126. [PubMed: 16045910]
140. Saxena T, and Bellamkonda RV (2015). A sensor web for neurons. Nat. Mater 14, 1190–1191. [PubMed: 26585085]
141. Fried I, Wilson CL, Maidment NT, Engel J, Behnke E, Fields TA, Macdonald KA, Morrow JW, and Ackerson L (1999). Cerebral microdialysis combined with single-neuron and electroencephalographic recording in neurosurgical patients. J. Neurosurg 91, 697–705. [PubMed: 10507396]
142. Yan W, Dong C, Xiang Y, Jiang S, Leber A, Loke G, Xu W, Hou C, Zhou S, Chen M, et al. (2020). Thermally drawn advanced functional fibers: New frontier of flexible electronics. Mater. Today, DOI: 10.1016/j.mattod.2019.1011.1006.
143. Kozai TDY, Jaquins-Gerstl AS, Vazquez AL, Michael AC, and Cui XT (2015). Brain tissue responses to neural implants impact signal sensitivity and intervention strategies. ACS Chem. Neurosci 6, 48–67. [PubMed: 25546652]
144. Khodagholy D, Gelinas JN, and Buzsáki G (2017). Learning-enhanced coupling between ripple oscillations in association cortices and hippocampus. Science 358, 369–372. [PubMed: 29051381]
145. Park S, Frank JA, and Anikeeva P (2018). Silicon biointerfaces for all scales. Nat. Biomed. Eng 2, 471–472. [PubMed: 30948826]
146. Hong G, Fu TM, Qiao M, Viveros RD, Yang X, Zhou T, Lee JM, Park HG, Sanes JR, and Lieber CM (2018). A method for single-neuron chronic recording from the retina in awake mice. Science 360, 1447–1451. [PubMed: 29954976]
147. Tran NM, Shekhar K, Whitney IE, Jacobi A, Benhar I, Hong G, Yan W, Adiconis X, Arnold ME, Lee JM, et al. (2019). Single-Cell Profiles of Retinal Ganglion Cells Differing in Resilience to Injury Reveal Neuroprotective Genes. Neuron 104, 1039–1055.e1012. [PubMed: 31784286]
148. Barron KD (2003). Microglia: History, cytology, and reactions. J. Neurol. Sci 207, 98. [PubMed: 12614938]
149. McConnell GC, Rees HD, Levey AI, Gutekunst CA, Gross RE, and Bellamkonda RV (2009). Implanted neural electrodes cause chronic, local inflammation that is correlated with local neurodegeneration. J. Neural Eng 6, 056003. [PubMed: 19700815]
150. Schwartz M (2003). Macrophages and microglia in central nervous system injury: Are they helpful or harmful? J. Cerebr. Blood F. Met 23, 385–394.
151. Tsui C, Koss K, Churchward MA, and Todd KG (2019). Biomaterials and glia: Progress on designs to modulate neuroinflammation. Acta Biomater. 83, 13–28. [PubMed: 30414483]
152. Kim YT, Hitchcock RW, Bridge MJ, and Tresco PA (2004). Chronic response of adult rat brain tissue to implants anchored to the skull. Biomaterials 25, 2229–2237. [PubMed: 14741588]
153. Kastin A, and Schally A (1967). Autoregulation of Release of Melanocyte Stimulating Hormone from the Rat Pituitary. Nature 213, 1238–1240.
154. Galimberti D, Baron P, Meda L, Prat E, Scarpini E, Delgado R, Catania A, Lipton JM, and Scarlato G (1999). α-MSH peptides inhibit production of nitric oxide and tumor necrosis factor-α by microglial cells activated with β-amyloid and interferon γ. Biochem. Biophys. Res. Commun 263, 251–256. [PubMed: 10486285]
155. Zhong Y, and Bellamkonda RV (2005). Controlled release of anti-inflammatory agent α-MSH from neural implants. J. Control. Release 106, 309–318. [PubMed: 15978692]
156. Chao CC, Hu S, Close K, Choi CS, Molitor TW, Novick WJ, and Peterson PK (1992). Cytokine Release from Microglia: Differential Inhibition by Pentoxifylline and Dexamethasone. J. Infect. Dis 166, 847–853. [PubMed: 1527422]
157. Boehler C, Kleber C, Martini N, Xie Y, Dryg I, Stieglitz T, Hofmann UG, and Asplund M (2017). Actively controlled release of Dexamethasone from neural microelectrodes in a chronic in vivo study. Biomaterials 129, 176–187. [PubMed: 28343004]

158. Zhang Z, Nong J, and Zhong Y (2015). Antibacterial, anti-inflammatory and neuroprotective layer-by-layer coatings for neural implants. J. Neural Eng 12, 046015. [PubMed: 26052137]

159. Liu B, Kim E, Meggo A, Gandhi S, Luo H, Kallakuri S, Xu Y, and Zhang J (2017). Enhanced biocompatibility of neural probes by integrating microstructures and delivering anti-inflammatory agents via microfluidic channels. J. Neural Eng 14, 026008. [PubMed: 28155844]

160. Shaftel SS, Griffin WST, and O'Banion MK (2008). The role of interleukin-1 in neuroinflammation and Alzheimer disease: an evolving perspective. J. Neuroinflammation 5, 7. [PubMed: 18302763]

161. Taub AH, Hogri R, Magal A, Mintz M, and Shacham-Diamand Y (2012). Bioactive anti-inflammatory coating for chronic neural electrodes. J. Biomed. Mater. Res. A 100A, 1854–1858.

162. Levi-Montalcini R (1987). The Nerve Growth Factor 35 Years Later. Science 237, 1154–1162. [PubMed: 3306916]

163. Kennedy P (2012). A Prosthesis for Restoration of Speech in Locked-In Patients. Neurology 78, P02.003.

164. Kennedy PR, Andreasen DS, Bartels J, Ehirim P, Wright EJ, Seibert S, and Cervantes AJ (2018). Validation of Neurotrophic Electrode Long-Term Recordings in Human Cortex In Brain–Computer Interfaces Handbook: Technological and Theoretical Advances, Nam CS, Nijholt A and Lotte A, eds. (CRC Press), pp. 279–296.

165. Kennedy PR (1989). The cone electrode: a long-term electrode that records from neurites grown onto its recording surface. J. Neurosci. Methods 29, 181–193. [PubMed: 2796391]

166. Chen S, and Allen MG (2012). Extracellular matrix-based materials for neural interfacing. MRS Bull. 37, 606–613.

167. Hussey GS, Dziki JL, and Badylak SF (2018). Extracellular matrix-based materials for regenerative medicine. Nat. Rev. Mater 3, 159–173.

168. Ghuman H, Gerwig M, Nicholls FJ, Liu JR, Donnelly J, Badylak SF, and Modo M (2017). Long-term retention of ECM hydrogel after implantation into a sub-acute stroke cavity reduces lesion volume. Acta Biomater. 63, 50–63. [PubMed: 28917705]

169. Heiduschka P, Romann I, Ecken H, Schöning M, Schuhmann W, and Thanos S (2001). Defined adhesion and growth of neurones on artificial structured substrates. Electrochim. Acta 47, 299–307.

170. He W, McConnell GC, and Bellamkonda RV (2006). Nanoscale laminin coating modulates cortical scarring response around implanted silicon microelectrode arrays. J. Neural Eng 3, 316–326. [PubMed: 17124336]

171. Lee CD, Hara SA, Yu L, Kuo JTW, Kim BJ, Hoang T, Pikov V, and Meng E (2016). Matrigel coatings for Parylene sheath neural probes. J. Biomed. Mater. Res. B 104, 357–368.

172. Bai W, Shin J, Fu R, Kandela I, Lu D, Ni X, Park Y, Liu Z, Hang T, Wu D, et al. (2019). Bioresorbable photonic devices for the spectroscopic characterization of physiological status and neural activity. Nat. Biomed. Eng 3, 644–654. [PubMed: 31391594]

173. Kang S-K, Murphy RKJ, Hwang S-W, Lee SM, Harburg DV, Krueger NA, Shin J, Gamble P, Cheng H, Yu S, et al. (2016). Bioresorbable silicon electronic sensors for the brain. Nature 530, 71–76. [PubMed: 26779949]

174. Seo D, Neely RM, Shen K, Singhal U, Alon E, Rabaey JM, Carmena JM, and Maharbiz MM (2016). Wireless Recording in the Peripheral Nervous System with Ultrasonic Neural Dust. Neuron 91, 529–539. [PubMed: 27497221]

175. Piech DK, Johnson BC, Shen K, Ghanbari MM, Li KY, Neely RM, Kay JE, Carmena JM, Maharbiz MM, and Muller R (2020). A wireless millimetre-scale implantable neural stimulator with ultrasonically powered bidirectional communication. Nat. Biomed. Eng 4, 207–222. [PubMed: 32076132]

176. Wu X, Zhu X, Chong P, Liu J, Andre LN, Ong KS, Brinson K Jr., Mahdi AI, Li J, Fenno LE, et al. (2019). Sono-optogenetics facilitated by a circulation-delivered rechargeable light source for minimally invasive optogenetics. Proc. Natl. Acad. Sci. USA 116, 26332–26342.

177. Opie NL, John SE, Rind GS, Ronayne SM, Wong YT, Gerboni G, Yoo PE, Lovell TJH, Scordas TCM, Wilson SL, et al. (2018). Focal stimulation of the sheep motor cortex with a chronically

implanted minimally invasive electrode array mounted on an endovascular stent. Nat. Biomed. Eng 2, 907–914. [PubMed: 31015727]

178. Raducanu BC, Yazicioglu RF, Lopez CM, Ballini M, Putzeys J, Wang S, Andrei A, Rochus V, Welkenhuysen M, van Helleputte N, et al. (2017). Time multiplexed active neural probe with 1356 parallel recording sites. Sensors 17, 2388.
179. Steinmetz NA, Koch C, Harris KD, and Carandini M (2018). Challenges and opportunities for large-scale electrophysiology with Neuropixels probes. Curr. Opin. Neurobiol 50, 92–100. [PubMed: 29444488]
180. Owen SF, Liu MH, and Kreitzer AC (2019). Thermal constraints on in vivo optogenetic manipulations. Nat. Neurosci 22, 1061–1065. [PubMed: 31209378]
181. Fang Y, Meng L, Prominski A, Schaumann EN, Seebald M, and Tian B (2020). Recent advances in bioelectronics chemistry. Chem. Soc. Rev, DOI: 10.1039/D1030CS00333F.
182. Keene ST, Lubrano C, Kazemzadeh S, Melianas A, Tuchman Y, Polino G, Scognamiglio P, Cinà L, Salleo A, van de Burgt Y, et al. (2020). A biohybrid synapse with neurotransmitter-mediated plasticity. Nat. Mater, DOI: 10.1038/s41563-41020-40703-y.
183. Cramer T (2020). Learning with brain chemistry. Nat. Mater, DOI: 10.1038/s41563-41020-40711-y.
184. Fuller EJ, Keene ST, Melianas A, Wang Z, Agarwal S, Li Y, Tuchman Y, James CD, Marinella MJ, Yang JJ, et al. (2019). Parallel programming of an ionic floating-gate memory array for scalable neuromorphic computing. Science 364, 570–574. [PubMed: 31023890]
185. Sangwan VK, and Hersam MC (2020). Neuromorphic nanoelectronic materials. Nat. Nanotechnol 15, 517–528. [PubMed: 32123381]
186. Xia Q, and Yang JJ (2019). Memristive crossbar arrays for brain-inspired computing. Nat. Mater 18, 309–323. [PubMed: 30894760]
187. Park H-L, Lee Y, Kim N, Seo D-G, Go G-T, and Lee T-W (2020). Flexible Neuromorphic Electronics for Computing, Soft Robotics, and Neuroprosthetics. Adv. Mater 32, 1903558.

Highlights:

- Bioinspired sizes and morphologies enhance spatial resolution and multiplexing
- Reducing the interfacial mechanical mismatch increases chronic recording stability.
- Bioinspired topologies allow for conformal interfacing of various neural structures.
- Biochemical functionalization tempers immune response, improving chronic interfacing.

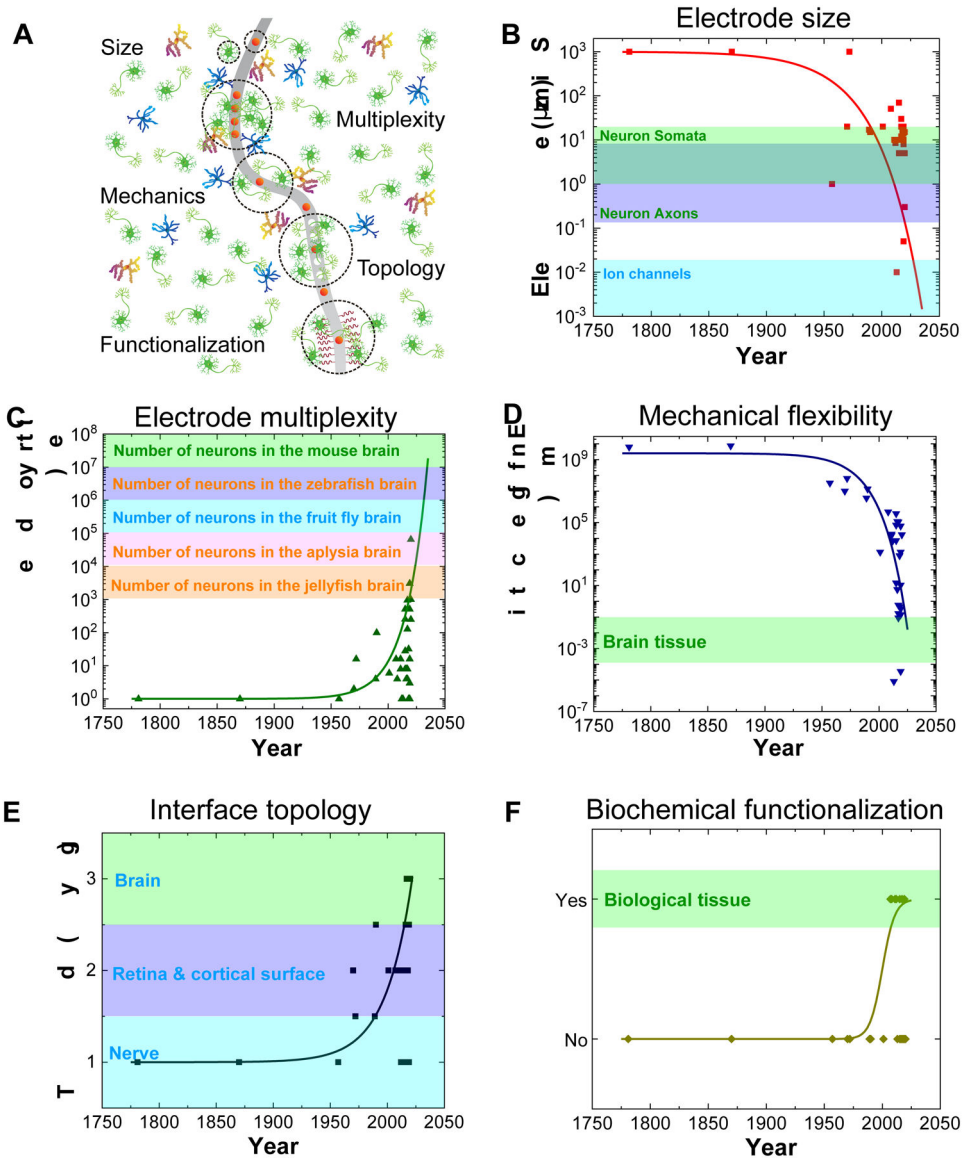

Figure 1.

Trends of *in vivo* bioelectronic neural interfaces with bioinspired size, multiplexity, mechanics, topology, and functionalization. (**A**) Schematic summarizing the bioinspired design features of *in vivo* bioelectronic neural interfaces. (**B**&**C**) The onset of modern fabrication techniques, such as photolithography, has made a substantial impact on the accessible resolution of device feature sizes, corresponding to a distinct decrease in electrode size (**B**), and an increase in electrode multiplexity, which is defined as the number of independent channels in a bioelectronic neural interface (**C**). The size ranges of typical neuronal structures[32–34] and the ranges of neuron number in different species[35–39] are shown in the colored shades of **B** and **C**, respectively. Note that the range of soma size (green shade) overlaps with that of axon size (blue shade) in **B**. **(D)** Engineering devices with soft materials and specific structures allows the effective bending stiffness, which is defined as ratio of bending moment to the product of width and curvature of the neural

probe, to decrease by up to ten orders of magnitude, reducing the overall probability of eliciting a chronic immune response. The range of effective bending stiffness of a 20 – 100 μm thick slice of brain tissue is shown as the green shade.[18] **(E)** A general trend in the topology of neural interfaces is found towards higher dimensions, allowing for more intimate interfacing with the neural tissue due to brain-device conformability. Non-integer topologies, such as radially segmented DBS electrode array (1D – 2D) and Utah slanted electrode array (2D – 3D) are indicated due to variability in design. The dimensionality of different components of the nervous system is shown as colored shades. **(F)** Progression of the field towards biochemical functionalization represents another clear marker of bioinspired neural interfaces. Biological tissues are intrinsically functionalized with biochemical cues, as labeled in the colored shade. In all graphs, solid curves are intended to guide the visualization of trends of various important features of bioelectronic neural interfaces and are not intended to fit these data to a particular mathematical model, although a similar trend of exponential growth has been found for doubling of simultaneously recorded neurons and Moore's law.[18] All data points come from technologies listed in Table 1.

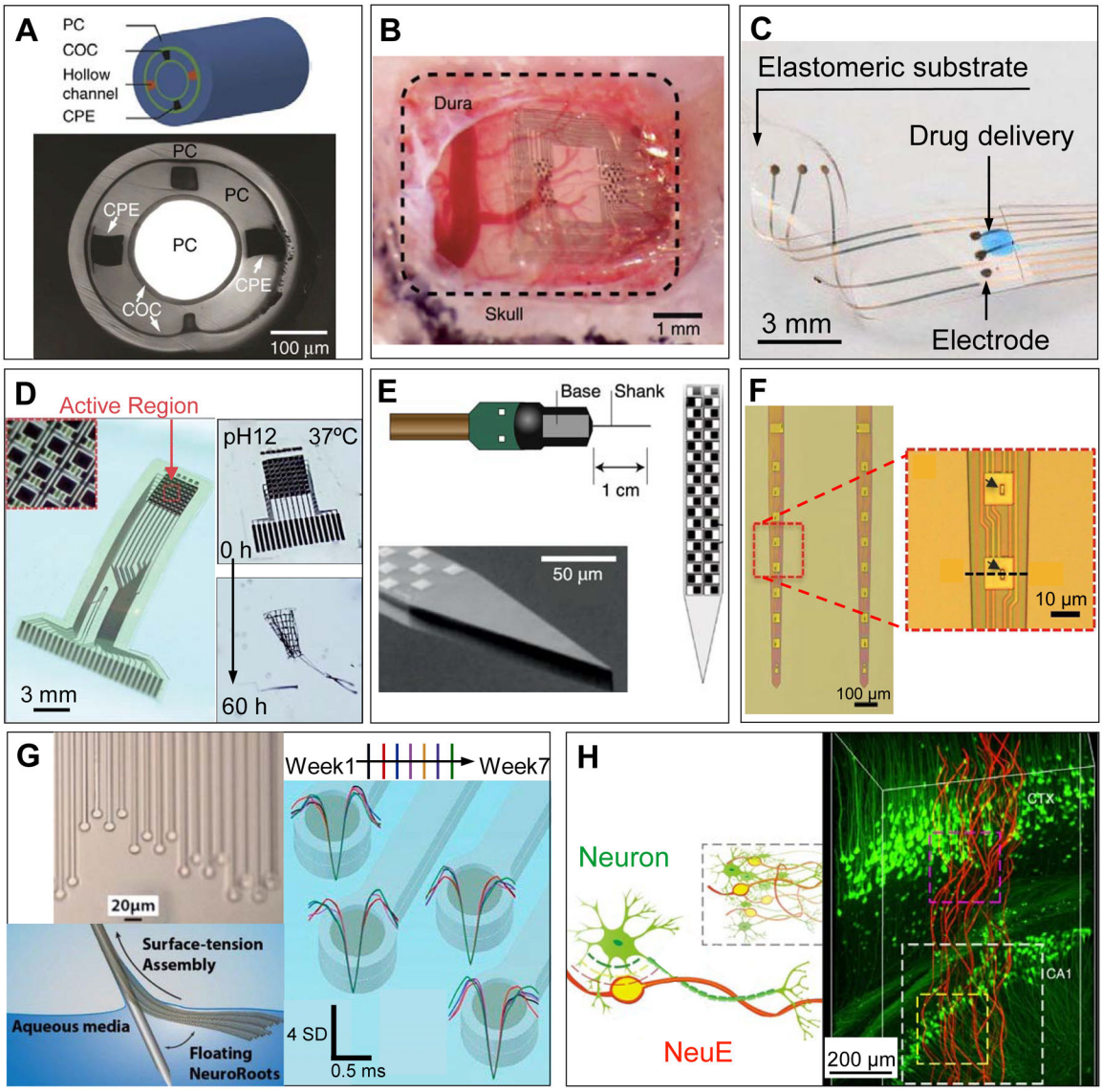

Figure 2.

Examples of novel *in vivo* bioelectronic neural interfaces. **(A)** Multifunctional fibers, constructed via thermal drawing processes, offer a multimodal means of interacting with neurons. As demonstrated in the schematic drawing (top) and a cross-sectional image (bottom) of the multifunctional fiber, this design incorporates one cylindrical optical waveguide comprising a polycarbonate (PC) core and a cyclic olefin copolymer (COC) shell, two microfluidic channels (‘hollow channels’) for local drug delivery, and two conductive polyethylene electrodes (CPE) for recording extracellular action potentials. Adapted with permission from Ref. 50. **(B)** NeuroGrid features poly(3,4-ethylenedioxythiophene) polystyrene sulfonate (PEDOT:PSS) coated electrodes with sizes and interelectrode spacing inspired by the average size of neuron somata and neuronal density within the neocortex, and is capable of resolving both local field potentials (LFPs) and single unit activity when conformally interfacing the curvilinear cortical surface. Adapted with permission from Ref. 52. **(C)** e-dura is designed to mimic the mechanical

properties of the dura mater of the brain and spinal cord. By integrating flexible silicone with thin films of conductive platinum-silicone composites and a microfluidic channel, the e-dura affords seamless integration with the spinal cord and potentially superficial regions of the brain, enabling electrical recording and stimulation in addition to local drug delivery. Adapted with permission from Ref. 51. **(D)** Bioresorbable silicon electronics are designed to seamlessly interface with cortical tissue for transient monitoring and modulation of brain activity (left). By integrating functional materials that can dissolve under physiological conditions, bioresorbable electronics show rapid dissolution upon immersion in an aqueous buffer solution with pH = 12 at 37 °C (right). Adapted with permission from Ref. 55. **(E)** Neuropixels facilitates electrophysiological recordings that demand high channel counts (left). Neuropixels incorporates 960 electrodes (layout shown in the right), with 384 active processing units at any one time. Adapted with permission from Ref. 57. **(F)** Ultraflexible nanoelectronic probes (shown: NET-50, left) combine reduced feature sizes of electrodes (right) and flexible materials to produce a device capable of chronically stable single unit recording. Adapted with permission from Ref. 56. **(G)** NeuroRoots takes inspiration from axon sizes and distribution within the brain (top left) and can be inserted into the brain through self-assembly, mediated by capillary forces, along the direction of the microwire shuttle (bottom left). Owing to NeuroRoots' flexibility and small footprint, stable single unit recording is demonstrated for up to 7 weeks (right). Adapted with permission from Ref. 61. (**H**) Neuron-like electronics (NeuE) combine bioinspired feature sizes, mechanical compliance and topological properties (left) to optimize device-brain interfacing (right) and affords chronic recording stability. Adapted with permission from Ref. 63.

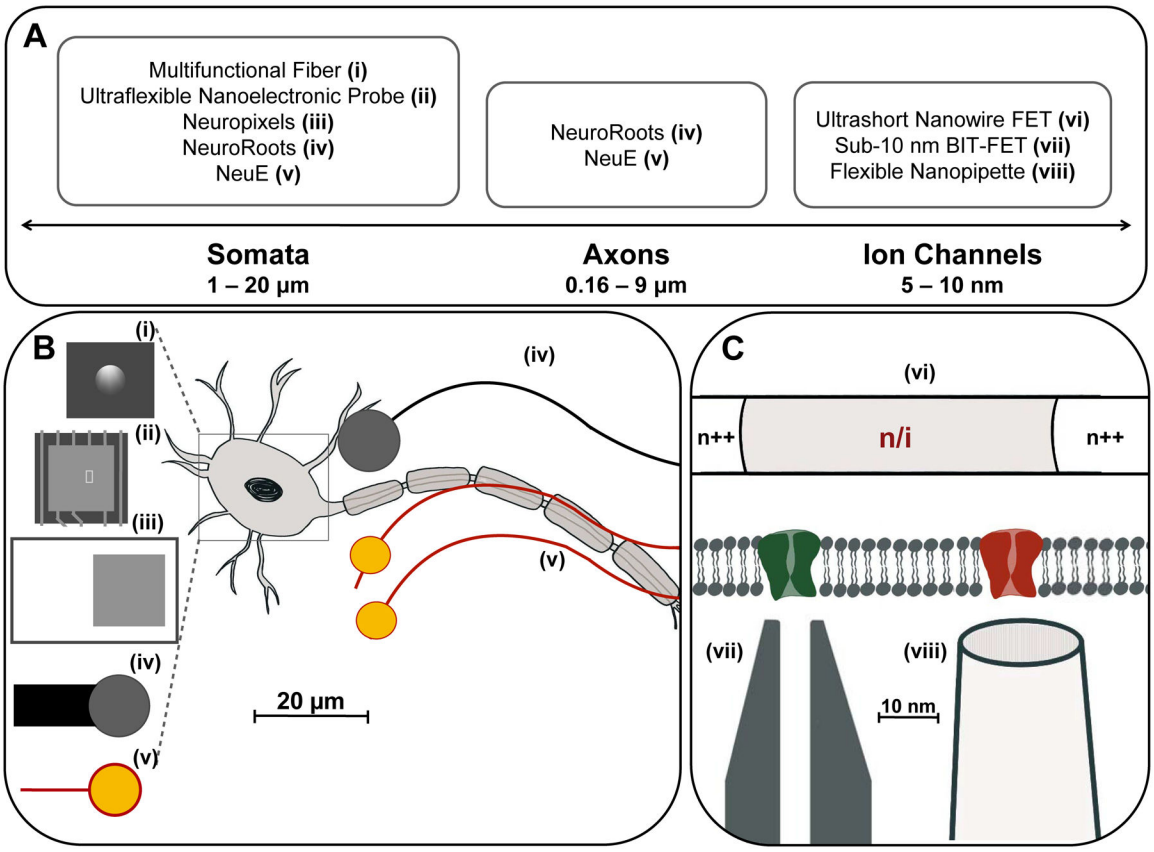

Figure 3.

Bioelectronic neural interfaces inspired by the size and morphology of neuron somata and neurites. (**A**) Feature sizes of the subcellular structures of the neuron, ranging from a few nanometers for ion channels, 0.16 – 9 microns for axonal diameter, to 1 – 20 microns for neuron somata. **(B)** Many modern bioelectronic neural interfaces have recording electrodes of similar sizes to neuron somata. Shown are the electrode regions of **(i)** Multifunctional fibers (d = 5 μm), **(ii)** Ultraflexible nanoelectronic probe (d = 10 μm), **(iii)** Neuropixels (d = 12 μm), **(iv)** NeuroRoots (d = 10 μm), **(v)** NeuE (d = 8 – 20 μm), where d is the diameter for round electrodes, or width for square electrodes. Additionally, by mimicking the size characteristics of axons, neural interfaces can encourage acceptance in the endogenous neural tissue via promotion of neural progenitor cell migration and integration with the neuronal network. Shown: **(iv)** NeuroRoots ($w \sim 7$ μm), **(v)** NeuE (w = 1 – 4 μm), where w is the width of interconnect ribbons in the electronics. **(C)** Devices mimicking the size of ion channels, such as the 50 nm ultrashort-channel FET and sub-10 nm BIT-FET, allow recording from individual ion channels with subcellular resolution. Shown: **(vi)** Ultrashort nanowire FET, **(vii)** Sub-10 nm BIT FET, and **(viii)** Flexible nanopipette.

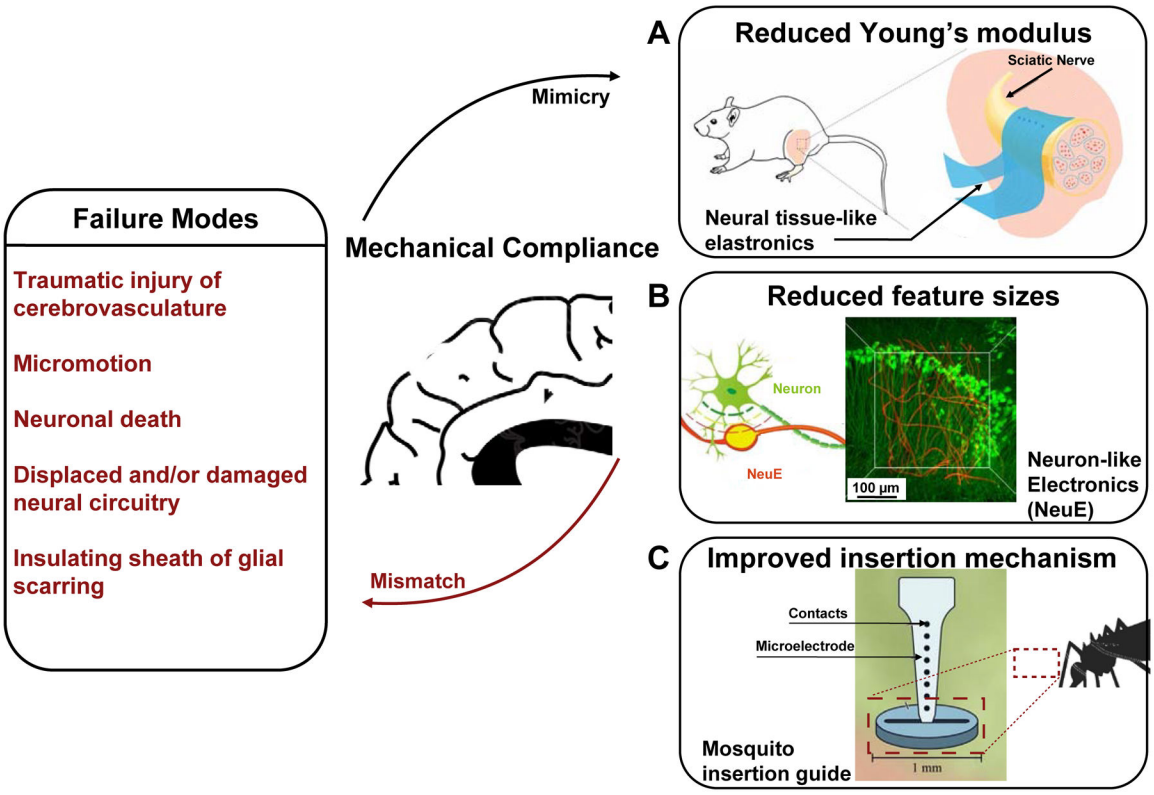

Figure 4.

Bioelectronic neural interfaces inspired by the mechanical properties of neural tissue. Bioinspired mechanical compliance may result from the reduction of **(A)** the material's Young's modulus, through engineering thin-film hydrogel elastronics with Young's moduli on the order of kPa, or **(B)** feature sizes, with neuron-like electronics (NeuE). A schematic of the intertwined neuron-NeuE interface is shown on the left, and a reconstructed 3D image of neurons (green) interpenetrating the electronic network of NeuE (red) in shown on the right. Finally, improved insertion mechanisms of flexible neural interfaces may be realized through a variety of bioinspired strategies, such as the fascicles of female mosquitos, thereby reducing buckling during implantation **(C)**. Reproduced with permission from Refs. 63, 110, 112.

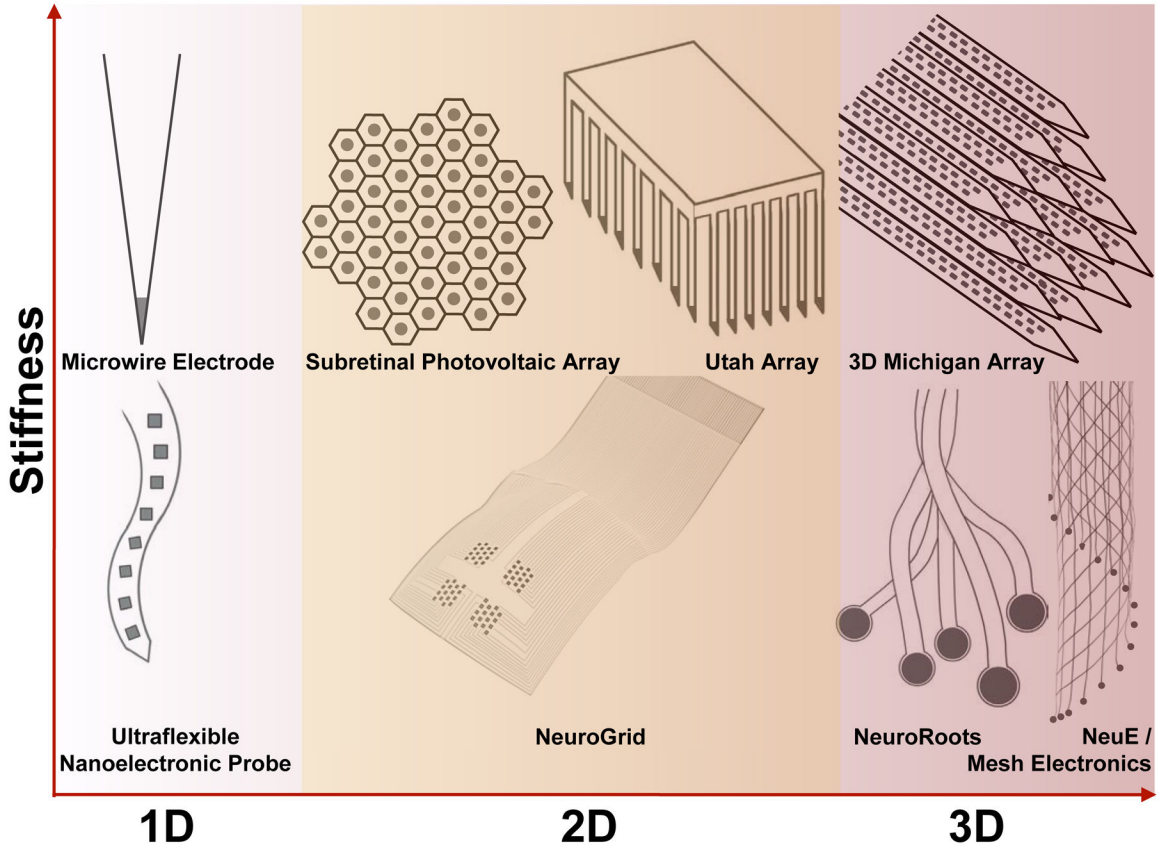

Figure 5.

Bioelectronic neural interfaces inspired by the topology of neural tissue. This means that, for neurons within the brain (white-red gradient), neural interfaces constantly advance toward 3D topologies. Starting with the microwire electrode, silicon-based fabrication strategies ignited arraying rigid materials for higher-dimensional interfacing, as seen with the Utah array and the 3D Michigan array. In contrast, interrogation of the neurons in the retina (i.e., retinal ganglion cells) and on the cortical surface requires interfacing at two dimensions on a curvilinear surface (yellow highlight in the middle column). Meanwhile, the joint trend towards higher-dimensional topologies is maintained for flexible bioelectronic neural interfaces, evidenced by the ultraflexible nanoelectronic probe (NET-50), NeuroGrid, NeuroRoots, mesh electronics, and NeuE. Dark gray circles and squares indicate recording sites in these examples. Schematics are not to scale in these drawings.

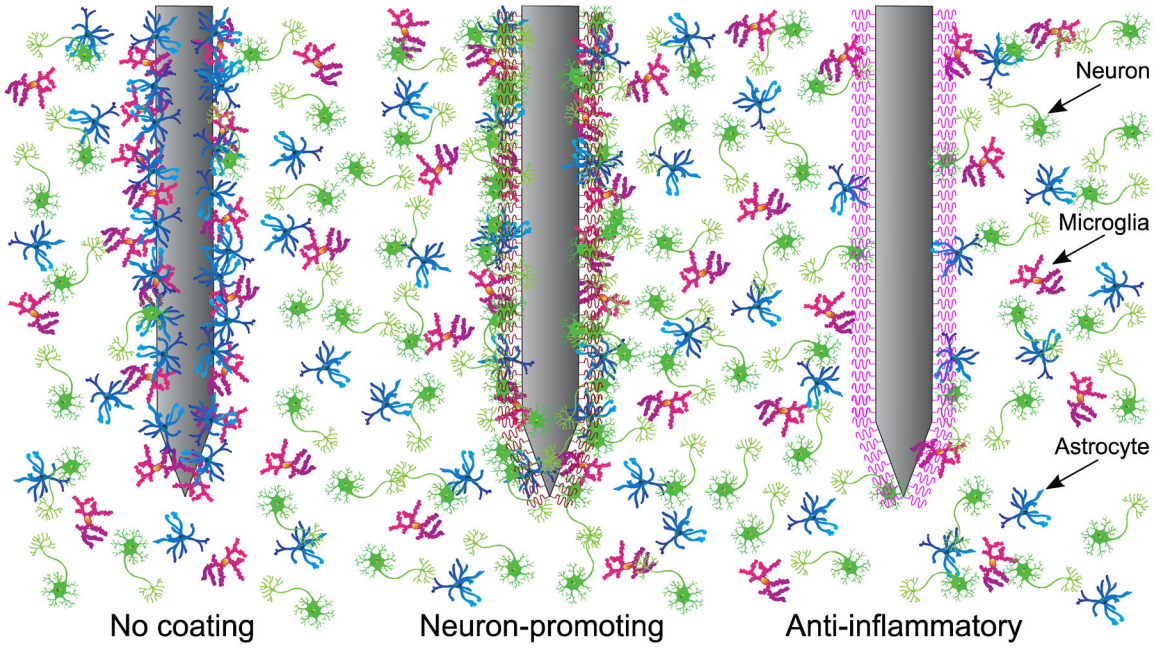

Figure 6.

Bioelectronic neural interfaces with bioinspired functionalization. At left, a typical immune response to a non-coated neural implant is illustrated. Astrocytes and microglia accumulate at the probe interface, ultimately forming a glial scar, and neuronal loss is observed around the probe. At center, a probe with neuron-promoting coating (such as L1 or Matrigel) prevents local neural loss while reducing immune response, thoroughly incorporating the probe with the endogenous neural tissue. At right, an interface with anti-inflammatory coating (such as α-MSH or IL1-receptor antagonist) significantly reduces the presence of microglia and astrocytes, allowing unhindered access to local neurons.

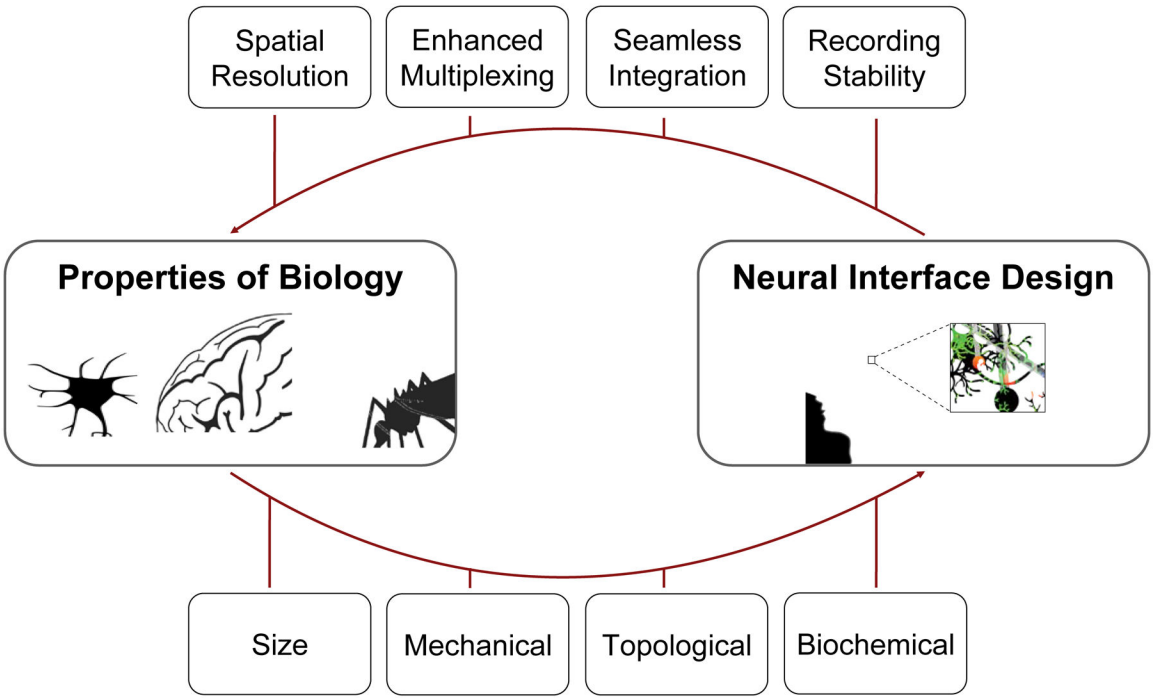

Figure 7.

Envisioned synergy between neuroscience, which elucidates the properties of biology in the nervous system, and neuroengineering, via neural interface design. In particular, the knowledge of the size, mechanical, topological, and biochemical properties of the brain affords an unprecedented opportunity for next-generation neural interface design, with features such as high spatiotemporal resolution, enhanced electrode multiplexity (i.e., number of electrodes), the capability for seamless integration, and chronic recording stability.

Table 1.

Historical, conventional and novel bioelectronic neural interfaces.

Year of appearance	Bioelectronic neural interface	Reference
1781	Galvani bimetal arch wire	5
1870	Fritsch lead wire	6
1957	Hubel microwire	11
1970	Michigan array	19
1972	DBS electrode	40
1989	Tetrode	41
1990	Utah array	20
2001	Polyimide probe	42
2007	Michigan MEA with anti-inflammatory surface coating	43
2007	Dexamethane-coated Michigan MEA	44
2008	Neurotrophic electrode	45
2011	Neural probes coated with neuron-adhesion molecules	46
2011	Fish-bone-shaped neural probe	47
2012	Microthread electrode (MTE)	48
2013	Sub-10 nm BIT-FET	49
2015	Multifunctional fiber	50
2015	e-dura	51
2015	NeuroGrid array	52
2015	Subretinal photovoltaic array	53
2016	Endovascular stent-electrode	54
2016	Bioresorbable silicon electronics	55
2017	Ultraflexible nanoelectronic probes (“nanoelectronic threads”: NET-50, NET-10)	56
2017	Neuropixels	57
2017	Highly scalable mesh electronics	58
2018	Silicon nanoscale membrane	59
2018	Nanowire-based artificial photoreceptors	60
2018	NeuroRoots	61
2018	Carbon nanotube fiber microelectrodes (CNTf)	62
2019	Neuron-like electronics (NeuE)	63
2019	Neurotassels	64
2019	Flexible electrode threads (Neuralink)	65
2019	Integrated glass microelectrodes	17
2019	Polymer electrode array	66
2019	Flexible nanopipette	67
2019	U-shaped silicon nanowire transistor	68
2020	CMOS interfaced microwire array	69
2020	Neural Matrix	70

Year of appearance	Bioelectronic neural interface	Reference
2020	Enhancement-mode, internal ion-gated organic electrochemical transistor (e-IGT)	71
2020	Liquid retina prosthesis	72
2020	The Argo (a 65,536-channel neural recording system)	73